An anisotropic a priori error analysis for a convection–dominated diffusion problem using the HDG method

Rommel Bustinza[a,b,*], Ariel L. Lombardi[c,d], Manuel Solano[a,b]

[a] *Departamento de Ingeniería Matemática, Facultad de Ciencias Físicas y Matemáticas, Universidad de Concepción, Casilla 160-C, Concepción, Chile*
[b] *Centro de Investigación en Ingeniería Matemática (CI^{2}MA), Universidad de Concepción, Casilla 160-C, Concepción, Chile*
[c] *Member of CONICET, Argentina*
[d] *Departamento de Matemática, Facultad de Ciencias Exactas, Ingeniería y Agrimensura, Universidad Nacional de Rosario. Av. Pellegrini 250, 2000 Rosario, Argentina*

Abstract

This paper deals with the a priori error analysis for a convection-dominated diffusion 2D problem, when applying the HDG method on a family of anisotropic triangulations. It is known that in this case, boundary or interior layers may appear. Therefore, it is important to resolve these layers in order to recover, if possible, the expected order of approximation. In this work, we extend the use of HDG method on anisotropic meshes. To this end, some assumptions need to be asked to the stabilization parameter, as well as to the family of triangulations. In this context, when the discrete local spaces are polynomials of degree $k \geq 0$, this approach is able to recover an order of convergence $k + \frac{1}{2}$ in L^2 for all the variables. Numerical examples confirm our theoretical results.

Keywords: `Hybridizable Discontinuous Galerkin, convection-dominated diffusion problem, anisotropic meshes`

2010 MSC: 65N30; 65N12; 65N15

*Corresponding author

Email addresses: `rbustinz@ing-mat.udec.cl` (Rommel Bustinza), `ariel@fceia.unr.edu.ar` (Ariel L. Lombardi), `msolano@ing-mat.udec.cl` (Manuel Solano)

1. Introduction

The first studies of convection diffusion problems applying discontinuous Galerkin (DG) methods, on a shape-regular family of triangulations, are referred to [1, 2], in the early 2000. Since then, many other DG methods have been used for this kind of problem. For example, in [3, 4, 5, 6, 7, 8] the authors consider the local discontinuous Galerkin (LDG) methods, while the multiscale discontinuous Galerkin method (see [9] for an overview) is used in [10, 11]. The interior penalty discontinuous Galerkin (IP-DG) methods are applied in [12, 13], the method of Bauman and Oden is considered in [14], the mixed-hybrid DG method is employed in [15] and the HDG methods are used in [16, 17, 18, 19, 20, 21]. HDG methods are a brand new class of DG schemes, that have been used lately. We refer [22] for a description of the technique, when applies to a linear second order elliptic equation. One of the main advantages of HDG methods, as indicated in [22], is the fact that one just has to solve a linear system on the skeleton of the mesh, and then recover the rest of (global) unknowns via an element-by-element calculation.

On the other hand, the fact that the exact solution of this kind of problems may generate layers (cf. [23, 24]), makes difficult to obtain a good approximation of it close to the layers. This could affect the rate of convergence of the method, and it is in general improved after the layers are resolved. This improvement can be done by considering meshes whose elements are concentrated along the layers. To do this, we would need to know in advance if there are layers, and if so, where they are. Since we do not usually know the exact solution, one alternative is the development of a suitable a posteriori error estimate which let us to perform an adaptive procedure to the mesh in order to capture the layer. In [25] the authors propose a reliable and efficient a posteriori error estimate for a convection-dominated diffusion reaction problem, and include some numerical tests that validate the good behaviour and robustness of the estimator.

Concerning anisotropic meshes, we can refer to [26], where the authors present an LDG a priori error analysis of a 2D convection-dominated diffu-

sion problem using Shishkin quadrilateral meshes, when the exact solution has exponential boundary layers. Our aim is to develop HDG methods for a convection-dominated diffusion 2D problem, when considering a sequence of simplicial meshes which may contain anisotropic elements. It is known that anisotropic meshes should be best suited for this kind of problem.

However, in this situation, the regularity property of the meshes is no longer valid. Instead of this, we require that the meshes satisfy the *maximum angle condition* (cf. [27]). This would be the first HDG analysis in this direction, and from certain point of view, it generalizes the 2D a priori error analysis for a larger family of triangulations, when HDG method is applied. To this end, we follow ideas given in [12] and [19]. We remark at least two differences of our analysis with respect to [19]. First, the numerical vector flux we introduced is given in the sense of LDG scheme. Secondly, despite [19], we only need to consider the standard local L^2-orthogonal projection operators and their approximation properties on anisotropic triangles. As result, we deduce that $||u-u_h||_{\mathcal{T}}$, the L^2-norm of error $u-u_h$ in the triangulation $\mathcal{T}$, satisfies

$$\frac{1}{||\varphi||_h}||u\,-\,u_h||_{L^2(\Omega)}\,=\,\mathcal{O}(h^{k+0.5})\,,$$

once the layers have been resolved. Here, u is the exact solution, u_h its HDG-approximation, and φ is a suitable function that depends on $\mathcal{T}$, and whose norm can be bounded by ϵ^{-1}. Here, ϵ represents the diffusion coefficient, h is intended to be the mesh size considered to obtain u_h, that is, $h := \max\{h_K\,:\,K\in\mathcal{T}\}$, with h_K being the diameter of K. Additional symbols and notations will be properly introduced in Section 3.

The rest of the paper is organized as follows. In Section 2, we introduce the model problem, deduce the HDG formulation and discuss on its unique solvability. The details of the anisotropic a priori error analysis are given in Section 3. Next, in Section 4, several numerical examples are shown, whose results are in agreement with our convergence analysis, even in cases where the maximum angle is close to π. Finally, we end this work, giving some conclusions and final remarks.

2. Convection–diffusion problem

Here, we consider the model problem

$$\begin{aligned} \epsilon^{-1}\,\boldsymbol{q} + \nabla u &= 0 \quad \text{in } \Omega\,, \\ \boldsymbol{\sigma} &= \boldsymbol{q} + u\,\boldsymbol{v} \quad \text{in } \Omega\,, \\ \nabla\cdot\boldsymbol{\sigma} &= f \quad \text{in } \Omega\,, \\ u &= g \quad \text{on } \partial\Omega\,, \end{aligned} \tag{1}$$

where Ω is a polygonal domain in $\mathbb{R}^2$, $f \in L^2(\Omega)$, $g \in H^{1/2}(\partial\Omega)$, the convection velocity field $\boldsymbol{v} \in [W^{1,\infty}(\Omega)]^2$, and has neither closed curves nor stationary points. In addition, we require that $\nabla\cdot\boldsymbol{v} \geq 0$ in Ω. This implies (see [12], Appendix A, for a proof) that there exists a smooth function ψ so that $\boldsymbol{v}(\boldsymbol{x})\cdot\nabla\psi(\boldsymbol{x}) \geq b_0 \quad \forall\,\boldsymbol{x}\in\Omega$, for some constant $b_0 > 0$.

Remark 2.1. *When $\boldsymbol{v} \in [\mathcal{P}_0(\bar{\Omega})]^2$, we can set $\psi(\boldsymbol{x}) := b_0 \frac{\boldsymbol{v}\cdot\boldsymbol{x}}{||\boldsymbol{v}||^2}$.*

Now, in order to define the HDG method, we let $\mathcal{T}$ be a triangulation of $\overline{\Omega}$, made of triangular elements satisfying a maximum angle condition with constant $\tilde{\beta} < \pi$. This means that all the angles of the triangles in $\mathcal{T}$ are less or equal than $\tilde{\beta} > 0$ (see hypothesis **M.1** in Section 3). We remind that for any $K \in \mathcal{T}$, h_K denotes the diameter of K and $h := \max_{K\in\mathcal{T}} h_K$. We also introduce $\partial\mathcal{T} := \{\partial K\,:\,K\in\mathcal{T}\}$, and let $\mathcal{E}$ be the set of all sides F of all elements $K \in \mathcal{T}$, counted once. Given $K \in \mathcal{T}$, we denote by $\boldsymbol{n}$ the unit normal vector, exterior to ∂K. Concerning the approximation spaces, we first introduce the space of piecewise polynomials of degree at most $k \in \mathbb{N}\cup\{0\}$

$$P_k(\mathcal{T}) := \left\{ w \in L^2(\Omega)\,:\, w|_K \in P_k(K) \quad \forall\, K\in\mathcal{T} \right\}.$$

Then, we look for the approximation of u and $\boldsymbol{q}$ in the discrete spaces $W_h := P_k(\mathcal{T})$ and $\boldsymbol{V}_h := [P_k(\mathcal{T})]^2$, respectively. We also consider the space

$$M_h := P_k(\mathcal{E}) := \left\{ w \in L^2(\mathcal{E})\,:\, w|_F \in P_k(F) \quad \forall\, F\in\mathcal{E} \right\},$$

for another scalar unknown that lives on the skeleton of $\mathcal{T}$, well known as *numerical trace*, and the afine space

$$M_h(g) := \{\mu \in M_h : \langle \mu, \zeta \rangle_F = \langle g, \zeta \rangle_F \quad \forall\, \zeta \in P_k(F) \quad \forall\, F \in \mathcal{E} \cap \partial\Omega\},$$

for imposing Dirichlet boundary condition on the discrete formulation in a weak sense. Concerning the inner products consider here, all of them are piecewise defined. For instance,

$$(w, v)_{\mathcal{T}} := \sum_{K \in \mathcal{T}} \int_K w\, v \quad \forall\, w, v \in L^2(\Omega),$$

$$\langle \mu, \rho \rangle_{\partial\mathcal{T}} := \sum_{K \in \mathcal{T}} \int_{\partial K} \mu\, \rho \quad \forall\, \mu, \rho \in L^2(\partial\mathcal{T}).$$

The definition of $(\cdot,\cdot)_{\mathcal{T}}$ for vector functions is given in analogous way. By $||\cdot||_{\mathcal{T}}$ and $||\cdot||_{\partial\mathcal{T}}$ we denote the norms induced by the corresponding inner products defined above.

The HDG formulation reads as: Find $(\boldsymbol{\sigma}_h, \boldsymbol{q}_h, u_h, \widehat{u}_h) \in \boldsymbol{V}_h \times \boldsymbol{V}_h \times W_h \times M_h$, such that

$$\begin{aligned}
(\epsilon^{-1}\, \boldsymbol{q}_h, \boldsymbol{r})_{\mathcal{T}} - (u_h, \nabla \cdot \boldsymbol{r})_{\mathcal{T}} + \langle \boldsymbol{r} \cdot \boldsymbol{n}, \widehat{u}_h \rangle_{\partial\mathcal{T}} &= 0 && \forall\, \boldsymbol{r} \in \boldsymbol{V}_h, \\
(\boldsymbol{\sigma}_h, \boldsymbol{\rho})_{\mathcal{T}} - (\boldsymbol{q}_h, \boldsymbol{\rho})_{\mathcal{T}} - (u_h\, \boldsymbol{v}, \boldsymbol{\rho})_{\mathcal{T}} &= 0 && \forall\, \boldsymbol{\rho} \in \boldsymbol{V}_h, \\
-(\boldsymbol{\sigma}_h, \nabla w)_{\mathcal{T}} + \langle \widehat{\boldsymbol{\sigma}} \cdot \boldsymbol{n}, w \rangle_{\partial\mathcal{T}} &= (f, w)_{\mathcal{T}} && \forall\, w \in W_h, \\
\langle \widehat{u}_h, \mu \rangle_{\partial\Omega} &= \langle g, \mu \rangle_{\partial\Omega} && \forall\, \mu \in M_h, \\
\langle \widehat{\boldsymbol{\sigma}} \cdot \boldsymbol{n}, \mu \rangle_{\partial\mathcal{T} \setminus \partial\Omega} &= 0 && \forall\, \mu \in M_h,
\end{aligned} \tag{2}$$

where we set $\widehat{\boldsymbol{\sigma}} := \boldsymbol{q}_h + u_h\, \boldsymbol{v} + \tau(u_h - \widehat{u}_h)\boldsymbol{n}$ on $\partial\mathcal{T}$. Here we assume that $\tau \in P_0(\mathcal{E})$ is a non-negative parameter on $\mathcal{E}$.

We deduce from the second equation in (2) that $\boldsymbol{\sigma}_h = \boldsymbol{q}_h + P_{\boldsymbol{V_h}}(u_h\, \boldsymbol{v}) \in \boldsymbol{V}_h$, with $P_{\boldsymbol{V}_h}$ being the L^2-projection operator onto $\boldsymbol{V}_h$.

Remark 2.2. *We notice that when $\boldsymbol{v} \in [P_0(\Omega)]^2$, we have that $u_h\, \boldsymbol{v} \in [P_k(\mathcal{T})]^2$, provided $u_h \in P_k(\mathcal{T})$. This allows us to set the numerical flux $\widehat{\boldsymbol{\sigma}} := \boldsymbol{\sigma}_h + \tau(u_h - \widehat{u}_h)\, \boldsymbol{n}$ on $\partial\mathcal{T}$, in the same spirit of LDG method.*

Then, we derive an equivalent HDG formulation, which reads: Find $(\boldsymbol{q}_h, u_h, \widehat{u}_h) \in \boldsymbol{V}_h \times W_h \times M_h$, such that

$$\begin{aligned}
(\epsilon^{-1}\,\boldsymbol{q}_h, \boldsymbol{r})_{\mathcal{T}} - (u_h, \nabla\cdot\boldsymbol{r})_{\mathcal{T}} + \langle \boldsymbol{r}\cdot\boldsymbol{n}, \widehat{u}_h\rangle_{\partial\mathcal{T}} &= 0\,,\\
-(\boldsymbol{q}_h, \nabla w)_{\mathcal{T}} - (u_h\boldsymbol{v}, \nabla w)_{\mathcal{T}} + \langle (\boldsymbol{q}_h + u_h\boldsymbol{v})\cdot\boldsymbol{n} + \tau(u_h - \widehat{u}_h), w\rangle_{\partial\mathcal{T}} &= (f, w)_{\mathcal{T}}\,,\\
\langle \widehat{u}_h, \mu\rangle_{\partial\Omega} &= \langle g, \mu\rangle_{\partial\Omega}\,,\\
\langle (\boldsymbol{q}_h + u_h\boldsymbol{v})\cdot\boldsymbol{n} + \tau(u_h - \widehat{u}_h), \mu\rangle_{\partial\mathcal{T}\setminus\partial\Omega} &= 0\,,
\end{aligned} \tag{3}$$

for any $(\boldsymbol{r}, w, \mu) \in \boldsymbol{V}_h \times W_h \times M_h$.

The existence and uniqueness of the solution of the HDG scheme (3) is established next. To this end, it is important the identity

$$(w\,\boldsymbol{v}, \nabla w)_{\mathcal{T}} = \left\langle \frac{1}{2}(\boldsymbol{v}\cdot\boldsymbol{n})w, w\right\rangle_{\partial\mathcal{T}} - \left(\frac{1}{2}(\nabla\cdot\boldsymbol{v})w, w\right)_{\mathcal{T}} \quad \forall\, w \in H^1(\mathcal{T})\,. \tag{4}$$

Theorem 2.1. *If $\tau + \frac{1}{2}\boldsymbol{v}\cdot\boldsymbol{n} > 0$ on $\partial\mathcal{T}$, then the HDG formulation* (3) *has one, and only one solution.*

Proof. Since the discrete scheme is linear and square, it is enough to prove that the associated homogeneous linear system

$$(\epsilon^{-1}\,\boldsymbol{q}_h, \boldsymbol{r})_{\mathcal{T}} - (u_h, \nabla\cdot\boldsymbol{r})_{\mathcal{T}} + \langle \boldsymbol{r}\cdot\boldsymbol{n}, \widehat{u}_h\rangle_{\partial\mathcal{T}} = 0\,, \tag{5}$$

$$-(\boldsymbol{q}_h, \nabla w)_{\mathcal{T}} - (u_h\boldsymbol{v}, \nabla w)_{\mathcal{T}} + \langle (\boldsymbol{q}_h + u_h\boldsymbol{v})\cdot\boldsymbol{n} + \tau(u_h - \widehat{u}_h), w\rangle_{\partial\mathcal{T}} = 0\,, \tag{6}$$

$$\langle \widehat{u}_h, \mu\rangle_{\partial\Omega} = 0\,, \tag{7}$$

$$\langle (\boldsymbol{q}_h + u_h\boldsymbol{v})\cdot\boldsymbol{n} + \tau(u_h - \widehat{u}_h), \mu\rangle_{\partial\mathcal{T}\setminus\partial\Omega} = 0\,, \tag{8}$$

for any $(\boldsymbol{r}, w, \mu) \in \boldsymbol{V}_h \times W_h \times M_h$, has only the trivial solution.

First, from (7) we deduce that $\widehat{u}_h = 0$ on $\partial\Omega$. Taking $\boldsymbol{r} := \boldsymbol{q}_h$, $w := u_h$ and $\mu := \widehat{u}_h$ in (5), (6) and (8), respectively, and taking into account (4), we deduce after suitable algebraic manipulations

$$(\epsilon^{-1}\,\boldsymbol{q}_h, \boldsymbol{q}_h)_{\mathcal{T}} + \left(\frac{1}{2}(\nabla\cdot\boldsymbol{v})\,u_h, u_h\right)_{\mathcal{T}} + \left\langle \left(\tau + \frac{1}{2}\boldsymbol{v}\cdot\boldsymbol{n}\right)(u_h - \widehat{u}_h), u_h - \widehat{u}_h\right\rangle_{\partial\mathcal{T}} = 0\,.$$

Now, since $\tau + \frac{1}{2}\boldsymbol{v}\cdot\boldsymbol{n} > 0$ on $\partial\mathcal{T}$, we deduce that $u_h = \widehat{u}_h$ on $\partial\mathcal{T}$ and $\boldsymbol{q}_h = \boldsymbol{0}$ in $\mathcal{T}$. When $\nabla\cdot\boldsymbol{v} > 0$ a.e. Ω, we have $u_h = 0$ in $\mathcal{T}$, and then $\widehat{u}_h = 0$ on $\partial\mathcal{T}$.

Otherwise, (5) implies that $\nabla u_h = \mathbf{0}$ in $\mathcal{T}$, so $u_h \in P_0(\mathcal{T})$. Since $u_h = \widehat{u}_h$ on $\mathcal{T}$, we conclude that $u_h \in P_0(\overline{\Omega})$. As $u_h = \widehat{u}_h = 0$ on $\partial\Omega$, we derive that $u_h = 0$ in $\overline{\Omega}$. Thus, we end the proof.

□

3. An anisotropic a priori error analysis

We adapt the technique described in [19] to our case. First, we recall and introduce some notations and requirements on the family of triangulation.

For each $K \in \mathcal{T}$, β_K denotes the maximum interior angle of K, $h_K := \max_{F\in\partial K} |F|$ and $h_{\min,K} := \min_{F\in\partial K} |F|$. Given one side F of $K \in \mathcal{T}$, $F^\perp$ denotes the height relative to F. We introduce the principal directions of K, denoted by $\boldsymbol{s}_1$ and $\boldsymbol{s}_2$ (with $||\boldsymbol{s}_1|| = ||\boldsymbol{s}_2|| = 1$), as the directions of the sides E_1 and E_2 of K, sharing the vertex of the maximum angle of K. In addition, we consider the standard multi-index notation $\alpha := (\alpha_1, \alpha_2) \in \mathbb{Z}_0^+ \times \mathbb{Z}_0^+$, with length $|\alpha| := \alpha_1 + \alpha_2$, and define

$$\begin{aligned} \partial^\alpha &:= \partial_{\boldsymbol{s}_1}^{\alpha_1}\, \partial_{\boldsymbol{s}_2}^{\alpha_2} \quad \forall\, \alpha := (\alpha_1, \alpha_2) \in \mathbb{Z}_0^+ \times \mathbb{Z}_0^+\,, \\ \tilde{h}_K^\gamma &:= h_{1,K}^{\gamma_1}\, h_{2,K}^{\gamma_2} \quad \forall\, \gamma := (\gamma_1, \gamma_2) \in \mathbb{R} \times \mathbb{R}\,. \end{aligned} \tag{9}$$

Here, given $\boldsymbol{s}$ a unit vector, $\partial_{\boldsymbol{s}}$ denotes the corresponding derivative operator with respect to the direction $\boldsymbol{s}$, while $h_{1,K}$ and $h_{2,K}$ denote the lengths of E_1 and E_2, respectively.

From now on, we assume that $T := \{\mathcal{T}_m\}$ is a sequence of meshes that satisfies:

M.1 the *maximum angle condition*, i.e. there is $0 < \tilde{\beta} < \pi$ such that $\beta_K \le \tilde{\beta}$, $\forall\, K \in \mathcal{T}\,, \forall\, \mathcal{T} \in T$.

We recall here that we are not assuming the shape-regularity hypothesis, so our family of meshes may contain arbitrary anisotropic elements satisfying the maximum angle condition. Hereafter, we remark that C, with or without subscript or tildes, will denote a positive constant, that is independent of ϵ, the mesh size, and the maximum angle of any triangle of $\mathcal{T}$.

In what follows we consider that the parameter τ satisfies the following properties, for any $\mathcal{T} \in T$:

H.1 $\exists\, C_0 > 0$ such that $\max_{F\in\partial K} \tau|_F =: \tau_K^{max} \leq C_0$, $\forall\, K \in \mathcal{T}$.

H.2 $\exists\, C_1 > 0$ such that $\tau_K^{\boldsymbol{v}} := \max_{F\in\partial K} \inf_F \left(\tau + \frac{1}{2}\boldsymbol{v}\cdot\boldsymbol{n}\right) \geq C_1 \min\left\{\frac{\epsilon}{h_{\min,K}}, 1\right\}$, $\forall\, K \in \mathcal{T}$.

H.3 $\exists\, C_2 > 0$ such that $\inf_F \left(\tau + \frac{1}{2}\boldsymbol{v}\cdot\boldsymbol{n}\right) \geq C_2 \max_F |\boldsymbol{v}\cdot\boldsymbol{n}|$, $\forall\, F \in \partial K$, $\forall\, K \in \mathcal{T}$.

From now on, by $a \lesssim b$ we mean that $a \leq C\, b$, for some positive constant C that is independent of the mesh size and $\tilde{\beta}$.

We also need to consider the following broken Sobolev spaces

$$\boldsymbol{V}(\mathcal{T}) := [H^1(\mathcal{T})]^2 \quad , \quad W(\mathcal{T}) := H^1(\mathcal{T}) \quad , \quad M(\mathcal{E}) := L^2(\mathcal{E})\,.$$

Next, we introduce the bilinear form $B : (\boldsymbol{V}(\mathcal{T}) \times W(\mathcal{T}) \times M(\mathcal{E})) \times (\boldsymbol{V}(\mathcal{T}) \times W(\mathcal{T}) \times M(\mathcal{E})) \to \mathbb{R}$ given by

$$\begin{aligned} B((\boldsymbol{q},u,\lambda),(\boldsymbol{r},w,\mu)) \;:=\; & (\epsilon^{-1}\,\boldsymbol{q},\boldsymbol{r})_{\mathcal{T}} - (u,\nabla\cdot\boldsymbol{r})_{\mathcal{T}} + \langle \boldsymbol{r}\cdot\boldsymbol{n},\lambda\rangle_{\partial\mathcal{T}} - (\boldsymbol{q} + u\,\boldsymbol{v},\nabla w)_{\mathcal{T}} \\ & + \langle (\boldsymbol{q} + u\,\boldsymbol{v})\cdot\boldsymbol{n} + \tau\,(u-\lambda)\,,\, w-\mu\rangle_{\partial\mathcal{T}}\,, \end{aligned} \tag{10}$$

for any $(\boldsymbol{q},u,\lambda)\,,\,(\boldsymbol{r},w,\mu) \in \boldsymbol{V}(\mathcal{T}) \times W(\mathcal{T}) \times M(\mathcal{E})$. We notice that problem (3) can be written as: Find $(\boldsymbol{q}_h,u_h,\widehat{u}_h) \in \boldsymbol{V}_h \times W_h \times M_h(g)$ such that

$$B((\boldsymbol{q}_h,u_h,\widehat{u}_h),(\boldsymbol{r},w,\mu)) = (f,w)_{\mathcal{T}} + \langle g\,,\,\mu\rangle_{\partial\Omega} \quad \forall\,(\boldsymbol{r},w,\mu) \in \boldsymbol{V}_h \times W_h \times M_h(0)\,. \tag{11}$$

In what follows, we restrict ourselves, for simplicity, to the case $g = 0$ on $\partial\Omega$. Now, taking $(\boldsymbol{r},w,\mu) := (\boldsymbol{q}_h,u_h,\widehat{u}_h) \in \boldsymbol{V}_h \times W_h \times M_h(0)$, we deduce

$$||\epsilon^{-1/2}\boldsymbol{q}_h||_{\mathcal{T}}^2 + \left\|\left(\tau + \frac{1}{2}\boldsymbol{v}\cdot\boldsymbol{n}\right)^{1/2}(u_h - \widehat{u}_h)\right\|_{\partial\mathcal{T}}^2 + \left\|\left(\frac{1}{2}(\nabla\cdot\boldsymbol{v})\right)^{1/2} u_h\right\|_{\mathcal{T}}^2 = (f,u_h)_{\mathcal{T}}\,.$$

Unfortunately, if $\boldsymbol{v}$ is divergence-free, we do not have any control of the L^2-norm of u_h, by the standard energy argument. This motivates us to proceed as in [12]

(see also [19]). Then, we introduce the norm $|||\cdot||| : \boldsymbol{V}(\mathcal{T}) \times W(\mathcal{T}) \times M(\mathcal{E}) \to \mathbb{R}_0^+$, given by

$$|||(\boldsymbol{r}, w, \mu)|||^2 := ||\epsilon^{-1/2}\boldsymbol{r}||_{\mathcal{T}}^2 + ||w||_{\mathcal{T}}^2 + \sum_{K\in\mathcal{T}} \left\| \left(\frac{h_K}{h_{\min,K}}\right)^{1/2} \left(\tau + \frac{1}{2}\boldsymbol{v}\cdot\boldsymbol{n}\right)^{1/2} (w-\mu) \right\|_{\partial K}^2 ,$$

for any $(\boldsymbol{r}, w, \mu) \in \boldsymbol{V}(\mathcal{T}) \times W(\mathcal{T}) \times M(\mathcal{E})$. Next, we consider the function

$$\varphi_{\mathcal{T}} := \mathrm{e}^{-\psi} + \chi \max_{K\in\mathcal{T}} \left(\frac{h_K}{h_{\min,K}}\right) ,$$

where ψ is the function introduced at the beginning of Section 2, and χ is a (suitable) positive constant at our disposal. Then, we can establish the following result

Lemma 3.1. *Let $\varphi := \varphi_{\mathcal{T}}$ given above, with*

$$\chi \geq 1 + b_0^{-1} \, ||\nabla\psi||_{L^\infty(\Omega)}^2 \, ||\mathrm{e}^{-\psi}||_{L^\infty(\Omega)} \, ||\boldsymbol{v}||_{L^\infty(\Omega)} > 0 .$$

Assuming that $\tau + \frac{1}{2}\boldsymbol{v}\cdot\boldsymbol{n} > 0 \;\forall F \in \partial K, \forall K \in \mathcal{T}$, there exists $C > 0$, independent of ϵ and the mesh size, but depending on b_0, ψ and $\boldsymbol{v}$, such that

$$B((\boldsymbol{r}, w, \mu), (\boldsymbol{r}_\varphi, w_\varphi, \mu_\varphi)) \geq C \, |||(\boldsymbol{r}, w, \mu)|||^2 \quad \forall (\boldsymbol{r}, w, \mu) \in \boldsymbol{V}_h \times W_h \times M_h(0) ,$$

where $(\boldsymbol{r}_\varphi, w_\varphi, \mu_\varphi) := (\varphi\,\boldsymbol{r}, \varphi\, w, \varphi\,\mu)$.

Proof. Given $(\boldsymbol{r}, w, \mu) \in \boldsymbol{V}_h \times W_h \times M_h(0)$, we have, after integrating by parts and doing algebraic manipulations

$$B((\boldsymbol{r}, w, \mu), (\boldsymbol{r}_\varphi, w_\varphi, \mu_\varphi)) = (\epsilon^{-1}\boldsymbol{r}, \varphi\,\boldsymbol{r})_{\mathcal{T}} + (w\,,\, \mathrm{e}^{-\psi}\,\nabla\psi\cdot\boldsymbol{r})_{\mathcal{T}} + \frac{1}{2}((\nabla\cdot\boldsymbol{v})\,w\,,\,\varphi\,w)_{\mathcal{T}}$$

$$+ \frac{1}{2}((\boldsymbol{v}\cdot\nabla\psi)\,w\,,\,\mathrm{e}^{-\psi}\,w)_{\mathcal{T}} + \left\langle \left(\tau + \frac{1}{2}\boldsymbol{v}\cdot\boldsymbol{n}\right)\varphi\,(w-\mu)\,,\, w-\mu \right\rangle_{\partial\mathcal{T}} \tag{12}$$

Since $\boldsymbol{v}\cdot\nabla\psi \geq b_0 > 0$, $\nabla\cdot\boldsymbol{v} \geq 0$, and $\varphi \geq \chi \max_{K\in\mathcal{T}} \left(\frac{h_K}{h_{\min,K}}\right) \geq \chi$ in Ω, we deduce

$$B((\boldsymbol{r}, w, \mu), (\boldsymbol{r}_\varphi, w_\varphi, \mu_\varphi)) \geq \chi\,(\epsilon^{-1}\boldsymbol{r}, \boldsymbol{r})_{\mathcal{T}} + (w\,,\, \mathrm{e}^{-\psi}\,\nabla\psi\cdot\boldsymbol{r})_{\mathcal{T}} + \frac{b_0}{2}(w\,,\,\mathrm{e}^{-\psi}\,w)_{\mathcal{T}}$$

$$+ \chi \left\langle \max_{K\in\mathcal{T}} \left(\frac{h_K}{h_{\min,K}}\right) \left(\tau + \frac{1}{2}\boldsymbol{v}\cdot\boldsymbol{n}\right)(w-\mu)\,,\, w-\mu \right\rangle_{\partial\mathcal{T}} \tag{13}$$

Now, applying arithmetic-geometric Cauchy-Schwarz inequality, we have, for any $\delta > 0$,

$$\begin{aligned} 2\left|(w, \mathrm{e}^{-\psi}\,\nabla\psi\cdot\boldsymbol{r})_{\mathcal{T}}\right| &= 2\left|(\mathrm{e}^{-\psi/2}\,w, \mathrm{e}^{-\psi/2}\,\nabla\psi\cdot\boldsymbol{r})_{\mathcal{T}}\right| \\ &\leq \delta^{-1}(\mathrm{e}^{-\psi/2}\,\nabla\psi\cdot\boldsymbol{r}, \mathrm{e}^{-\psi/2}\,\nabla\psi\cdot\boldsymbol{r})_{\mathcal{T}}, + \delta\,(\mathrm{e}^{-\psi/2}\,w, \mathrm{e}^{-\psi/2}\,w)_{\mathcal{T}} \\ &\leq \delta^{-1}||\nabla\psi||^2_{L^\infty(\Omega)}\,(\mathrm{e}^{-\psi}\boldsymbol{r}, \boldsymbol{r})_{\mathcal{T}} + \delta\,(\mathrm{e}^{-\psi}\,w, w)_{\mathcal{T}} \\ &\leq \delta^{-1}||\nabla\psi||^2_{L^\infty(\Omega)}\,||\mathrm{e}^{-\psi}||_{L^\infty(\Omega)}\,||\boldsymbol{v}||_{L^\infty(\Omega)}\,(\epsilon^{-1}\boldsymbol{r}, \boldsymbol{r})_{\mathcal{T}} + \delta\,(\mathrm{e}^{-\psi}\,w, w)_{\mathcal{T}}\,, \end{aligned}$$

since $1 \ll \epsilon^{-1}\,||\boldsymbol{v}||_{L^\infty(\Omega)}$. This lets us to derive, from (13), that

$$B((\boldsymbol{r}, w, \mu), (\boldsymbol{r}_\varphi, w_\varphi, \mu_\varphi)) \geq \left(\chi - \frac{\delta^{-1}}{2}||\nabla\psi||^2_{L^\infty(\Omega)}||\mathrm{e}^{-\psi}||_{L^\infty(\Omega)}\,||\boldsymbol{v}||_{L^\infty(\Omega)}\right)(\epsilon^{-1}\boldsymbol{r}, \boldsymbol{r})_{\mathcal{T}}$$

$$+ \left(\frac{b_0}{2} - \frac{\delta}{2}\right)(w\,,\,\mathrm{e}^{-\psi}\,w)_{\mathcal{T}} + \chi\left\langle \max_{K\in\mathcal{T}}\left(\frac{h_K}{h_{\min,K}}\right)\left(\tau + \frac{1}{2}\boldsymbol{v}\cdot\boldsymbol{n}\right)(w-\mu)\,,\,w-\mu\right\rangle_{\partial\mathcal{T}}. \tag{14}$$

Choosing $\delta := b_0/2 > 0$ in (14), and taking into account the hypothesis on χ, we obtain

$$\begin{aligned} B((\boldsymbol{r}, w, \mu), (\boldsymbol{r}_\varphi, w_\varphi, \mu_\varphi)) &\geq (\epsilon^{-1}\boldsymbol{r}, \boldsymbol{r})_{\mathcal{T}} + \frac{b_0}{4}\,(\mathrm{e}^{-\psi}\,w\,,\,w)_{\mathcal{T}} \\ &\quad + \chi\left\langle \max_{K\in\mathcal{T}}\left(\frac{h_K}{h_{\min,K}}\right)\left(\tau + \frac{1}{2}\boldsymbol{v}\cdot\boldsymbol{n}\right)(w-\mu)\,,\,w-\mu\right\rangle_{\partial\mathcal{T}} \\ &\geq C\,|||(\boldsymbol{r}, w, \mu)|||^2\,, \end{aligned} \tag{15}$$

with $C > 0$ depending on b_0, $\mathrm{e}^{-\psi}$, $\nabla\psi$ and $\boldsymbol{v}$. □

We notice that the test function $(\boldsymbol{r}, w, \mu) := (\boldsymbol{r}_\varphi, w_\varphi, \mu_\varphi)$ in Lemma 16 does not belong to the discrete space $\boldsymbol{V}_h \times W_h \times M_h(0)$. In order to derive our a priori error estimate, we introduce the standard L^2-projection operators $\Pi_{\boldsymbol{V}}$, Π_W and P_M onto $\boldsymbol{V}_h$, W_h and M_h, respectively.

Another tool we need for the a priori error analysis, is the averaged Taylor operator Q_k of degree $k \geq 0$, introduced and analyzed in [28]. Indeed, given $u \in H^{k+1}(K)$, we define $Q_k u \in P_k(K)$ as

$$Q_k u(x) := \frac{1}{|K|}\int_K T_k u(y, x)\,dy\,,$$

with

$$T_k u(y,x) := \sum_{|\alpha|\le k} \partial^\alpha u(y) \frac{(y-x)^\alpha}{\alpha!} .$$

The approximation properties of Q_k are described next.

Lemma 3.2. *For any $K \in \mathcal{T}$ and any $w \in H^{k+1}(K)$, there exists $C > 0$, independent of the maximum angle β_K, such that for any side F of K with corresponding direction vector $\boldsymbol{s}$*

$$||w - Q_k w||_{L^2(K)} \le C \sum_{|\alpha|=k+1} \tilde{h}_K^\alpha ||\partial^\alpha w||_{L^2(K)} , \tag{16}$$

$$|F| \|\partial_{\boldsymbol{s}} Q_k w\|_{L^2(K)} \le C \, \|w\|_{L^2(K)} , \tag{17}$$

$$|F| \|\partial_{\boldsymbol{s}} (w - Q_k w)\|_{L^2(K)} \le C \sum_{|\alpha|=k+1} \tilde{h}_K^\alpha \|\partial^\alpha w\|_{L^2(K)} , \tag{18}$$

with $\tilde{h}_K^\alpha$ being defined as in (9).

Proof. These inequalities are obtained from [28], by rescaling arguments to a reference element. We omit further details. □

Next, we establish a geometric relation valid on any triangle.

Lemma 3.3. *For any triangle K there holds*

$$|F^\perp| \ge \frac{1}{2} \sin(\beta_K) \, h_{\min,K} \quad \forall \, F \in \partial K .$$

Proof. Let K be a triangle, and F_a, F_b and F_c its sides such that $|F_a| \le |F_b| \le |F_c|$. It is enough to prove the property for the height of K relative to its largest side. Then, we have

$$|F_c^\perp| \, |F_c| = 2 \, |K| = |F_a| \, |F_b| \, \sin(\beta_K) ,$$

with β_K denoting the maximum angle of K. The proof follows using the fact that

$$2 \, |F_b| \ge |F_b| + |F_a| > |F_c| .$$

We omit further details. □

In addition, we also need an anisotropic version of the trace inequality, which can be proven by standard rescaling arguments. We remark that in Lemma 2.3

in [29], it has been established an anisotropic trace inequality on tetrahedra, applying this kind of argument.

Lemma 3.4. *For any triangle $K \in \mathcal{T}$, there exists $C > 0$, independent of the mesh size and the maximum angle of K, such that for any side F of K, there holds*

$$||w||_{L^2(F)} \leq C\,|F^{\perp}|^{-1/2}\left(||w||_{L^2(K)} + \sum_{E\in\partial K}|E|\,||\partial_{\boldsymbol{s}_E} w||_{L^2(K)}\right), \quad \forall\, w \in H^1(K)\,,$$

where for any side E of K, $\boldsymbol{s}_E$ represents its unit direction vector.

The next result is a consequence of estimates for averaged Taylor operator.

Lemma 3.5. *Assume that $w \in H^{l_w+1}(K)$, for $l_w \in [0,k]$ on an element $K \in \mathcal{T}$. Then there exists $C > 0$, independent of the mesh size and the maximum angle β_K, such that*

$$||\Pi_W w - w||_{L^2(K)} \leq C \sum_{|\alpha|=l_w+1} \tilde{h}_K^{\alpha}\,||\partial^{\alpha} w||_{L^2(K)}\,.$$

Also, if $\boldsymbol{r} \in [H^{l_{\boldsymbol{r}}+1}(K)]^2$, for $l_{\boldsymbol{r}} \in [0,k]$ on an element $K \in \mathcal{T}$. Then there exists $C > 0$, independent of the mesh size and the maximum angle β_K, such that

$$||\Pi_{\boldsymbol{V}}\boldsymbol{r} - \boldsymbol{r}||_{[L^2(K)]^2} \leq C \sum_{|\alpha|=l_{\boldsymbol{r}}+1} \tilde{h}_K^{\alpha}\,||\partial^{\alpha}\boldsymbol{r}||_{L^2(K)]^2}\,,$$

with ∂^{α} and $\tilde{h}_K^{\alpha}$ being introduced in (9).

Proof. First, we consider the averaged Taylor approximation of w, $Q_k w \in P_k(K)$. Then, after noting that $\Pi_W(Q_k w) = Q_k w$ in K, we have

$$||\Pi_W w - w||_{L^2(K)} \leq ||\Pi_W(w - Q_k w)||_{L^2(K)} + ||Q_k w - w||_{L^2(K)} \leq 2\,||Q_k w - w||_{L^2(K)}\,.$$

The conclusion follows after applying (16). The second approximation property is proved in analogous way. □

Lemma 3.6. *Let $K \in \mathcal{T}$ and $\phi \in C^1(\bar{K}) \cap W^{k+1,\infty}(K)$. Then, for any $(\boldsymbol{r}, w) \in [P_k(K)]^2 \times P_k(K)$ and $\zeta \in \mathbb{R}$, there exists $C > 0$, such that*

$$\|(\Pi_{\boldsymbol{V}} - \boldsymbol{I})\,(\phi + \zeta)\,\boldsymbol{r}\|_{[L^2(K)]^2} \quad \leq \quad C\,\frac{h_K}{\sin(\beta_K)}\,||\phi||_{W^{k+1,\infty}(K)}\,||\boldsymbol{r}||_{[L^2(K)]^2}\,,$$

$$\|(\Pi_{\boldsymbol{V}} - \boldsymbol{I})\,(\phi + \zeta)\,\boldsymbol{r}\|_{[L^2(F)]^2} \;\leq\; C\,\frac{h_K^{1/2}}{\sin(\beta_K)}\left(\frac{h_K}{h_{\min,K}}\right)^{1/2} ||\phi||_{W^{k+1,\infty}(K)}\,||\boldsymbol{r}||_{[L^2(K)]^2} \quad \forall\, F \in \partial K\,,$$

$$\|(\Pi_W - I)\,(\phi + \zeta)\,w\|_{L^2(K)} \;\leq\; C\frac{h_K}{\sin(\beta_K)}\,||\phi||_{W^{k+1,\infty}(K)}\,||w||_{L^2(K)}\,,$$

$$\|(\Pi_W - I)\,(\phi + \zeta)\,w\|_{L^2(F)} \;\leq\; C\,\frac{h_K^{1/2}}{\sin(\beta_K)}\left(\frac{h_K}{h_{\min,K}}\right)^{1/2} ||\phi||_{W^{k+1,\infty}(K)}\,||w||_{L^2(K)} \quad \forall\, F \in \partial K\,.$$

Proof. Since $(\Pi_{\boldsymbol{V}} - \boldsymbol{I})((\phi+\zeta)\boldsymbol{r})|_K = (\Pi_{\boldsymbol{V}} - I)(\phi\boldsymbol{r})|_K$, and applying Lemma 3.5, we have

$$\begin{aligned}\|(\Pi_{\boldsymbol{V}} - \boldsymbol{I})(\phi+\zeta)\boldsymbol{r}\|_{[L^2(K)]^2} &\leq C\sum_{|\alpha|=k+1}\tilde{h}_K^{\alpha}\|\partial^{\alpha}(\phi\boldsymbol{r})\|_{[L^2(K)]^2}\\ &\leq C\sum_{|\alpha|=k+1}\tilde{h}_K^{\alpha}\sum_{\beta\leq\alpha}\|\partial^{\alpha-\beta}\phi\|_{L^\infty(K)}\|\partial^{\beta}\boldsymbol{r}\|_{[L^2(K)]^2}\end{aligned} \tag{19}$$

with the constant C from Lemma 3.5. Applying the inverse inequality

$$\|\partial^{\beta}\boldsymbol{r}\|_{[L^2(K)]^2} \leq \tilde{h}_K^{-\beta}\|\boldsymbol{r}\|_{[L^2(K)]^2}\,,$$

and taking into account that $\boldsymbol{r}$ is of degree less or equal than k, we obtain

$$\begin{aligned}\|(\Pi_{\boldsymbol{V}} - \boldsymbol{I})(\phi+\zeta)\boldsymbol{r}\|_{[L^2(K)]^2} &\leq \tilde{C}\,\csc(\beta_K)\,\|\phi\|_{W^{k+1,\infty}(K)}\sum_{|\alpha|=k+1}\sum_{\beta\leq\alpha,|\beta|\leq k}\tilde{h}_K^{\alpha-\beta}\|\boldsymbol{r}\|_{[L^2(K)]^2}\\ &\leq \tilde{C}\,\csc(\beta_K)\,h_K\|\phi\|_{W^{k+1,\infty}(K)}\|\boldsymbol{r}\|_{[L^2(K)]^2}\,,\end{aligned}$$

with $\tilde{C} > 0$ independent of the mesh size and the maximum angle of K. This concludes the proof of the first inequality.

To establish the second inequality, we take into account Lemma 3.4. Then, we obtain

$$\|(\Pi_{\boldsymbol{V}} - \boldsymbol{I})(\phi+\zeta)\boldsymbol{r}\|_{[L^2(F)]^2} = \|(\Pi_{\boldsymbol{V}} - \boldsymbol{I})(\phi\boldsymbol{r})\|_{[L^2(F)]^2}$$

$$\leq C\,|F^{\perp}|^{-1/2}\left(\|(\Pi_{\boldsymbol{V}} - \boldsymbol{I})(\phi\boldsymbol{r})\|_{[L^2(K)]^2} + \sum_{E\in\partial K}|E|\|\partial_{\boldsymbol{s}_E}(\Pi_{\boldsymbol{V}} - \boldsymbol{I})(\phi\boldsymbol{r})\|_{[L^2(K)]^2}\right). \tag{20}$$

Introducing now the averaged Taylor k-degree polynomial $Q_k(\phi\boldsymbol{r})$ of $\phi\boldsymbol{r}$ on K

and applying Lemma 3.2, we have

$$|E|\|\partial_{\boldsymbol{s}}(\Pi_{\boldsymbol{V}}-\boldsymbol{I})(\phi\boldsymbol{r})\|_{[L^2(K)]^2} = |E|\|\partial_{\boldsymbol{s}}(\Pi_{\boldsymbol{V}}-Q_k+Q_k-\boldsymbol{I})(\phi\boldsymbol{r})\|_{[L^2(K)]^2}$$

$$\leq |E|\|\partial_{\boldsymbol{s}}\left[Q_k(\Pi_{\boldsymbol{V}}-\boldsymbol{I})(\phi\boldsymbol{r})\right]\|_{[L^2(K)]^2} + |E|\|\partial_{\boldsymbol{s}_E}(Q_k-\boldsymbol{I})(\phi\boldsymbol{r})\|_{[L^2(K)]^2}$$

$$\leq C\left(\|(\Pi_{\boldsymbol{V}}-\boldsymbol{I})(\phi\boldsymbol{r})\|_{[L^2(K)]^2} + \sum_{|\alpha|=k+1}\tilde{h}_K^{\alpha}\|\partial^{\alpha}(\phi\boldsymbol{r})\|_{[L^2(K)]^2}\right). \tag{21}$$

Now, by the same argument used in equation (19) and from the first inequality of this Lemma, we deduce from (21)

$$|E|\|\partial_{\boldsymbol{s}_E}(\Pi_{\boldsymbol{V}}-\boldsymbol{I})(\phi\boldsymbol{r})\|_{[L^2(K)]^2} \leq C\,\csc(\beta_K)\,h_K\|\phi\|_{W^{k+1,\infty}(K)}\|\boldsymbol{r}\|_{[L^2(K)]^2},$$

and then, after replacing back in (20) and taking into account Lemma 3.3, we conclude that

$$\|(\Pi_{\boldsymbol{V}}-\boldsymbol{I})(\phi+\zeta)\boldsymbol{r}\|_{[L^2(F)]^2} \leq C\,\csc(\beta_K)\,h_{\min,K}^{-1/2}\,h_K\|\phi\|_{W^{k+1,\infty}(K)}\|\boldsymbol{r}\|_{[L^2(K)]^2},$$

with $C>0$ independent of the mesh size and the maximum angle β_K.

Third and fourth inequalities are proved analogously. □

In what follows, we set $||\varphi||_h := \max_{K\in\mathcal{T}}||\varphi||_{W^{k+1,\infty}(K)}$, and $D_{\tilde{\beta}} := \max_{K\in\mathcal{T}}\csc(\beta_K)$.

Lemma 3.7. *There exists $h_0>0$, independent of ϵ, but dependent of $\tilde{\beta}$, so that for any $h<h_0$, there holds the following inf-sup condition: There exists $C>0$, independent of ϵ, the maximum angle of all $K\in\mathcal{T}$ and the mesh size, such that for any $(\boldsymbol{q},u,\lambda)\in\boldsymbol{V}_h\times W_h\times M_h(0)$*

$$\sup_{\substack{(\boldsymbol{r},w,\mu)\in\boldsymbol{V}_h\times W_h\times M_h(0)\\(\boldsymbol{r},w,\mu)\neq(\boldsymbol{0},0,0)}}\frac{B((\boldsymbol{q},u,\lambda),(\boldsymbol{r},w,\mu))}{|||(\boldsymbol{r},w,\mu)|||} \geq \frac{C}{D_{\tilde{\beta}}\,||\varphi||_h}\,|||(\boldsymbol{q},\boldsymbol{u},\lambda)||| \tag{22}$$

Proof. First, we let $(\boldsymbol{q},u,\lambda)\in\boldsymbol{V}_h\times W_h\times M_h(0)$, and introduce $\boldsymbol{\delta q}_\varphi := (\boldsymbol{I}-\Pi_{\boldsymbol{V}})\boldsymbol{q}_\varphi\in\boldsymbol{V}(\mathcal{T})$, $\delta u_\varphi := (I-\Pi_W)u_\varphi\in W(\mathcal{T})$ and $\delta\lambda_\varphi := (I-P_M)\lambda_\varphi\in M(\mathcal{E})$. Then, we have

$$B((\boldsymbol{q},u,\lambda),(\boldsymbol{\delta q}_\varphi,\delta u_\varphi,\delta\lambda_\varphi)) = (\epsilon^{-1}\,\boldsymbol{q},\boldsymbol{\delta q}_\varphi)_{\mathcal{T}} - (u,\nabla\cdot\boldsymbol{\delta q}_\varphi)_{\mathcal{T}} + \langle\boldsymbol{\delta q}_\varphi\cdot\boldsymbol{n}\,,\,\lambda\rangle_{\partial\mathcal{T}}$$

$$
\begin{aligned}
& -(\boldsymbol{q} + u\,\boldsymbol{v}, \nabla\,\delta u_\varphi)_{\mathcal{T}} + \langle (\boldsymbol{q} + u\boldsymbol{v})\cdot\boldsymbol{n} + \tau(u-\lambda)\,,\,\delta u_\varphi\rangle_{\partial\mathcal{T}} \\
& -\langle (\boldsymbol{q} + u\boldsymbol{v})\cdot\boldsymbol{n} + \tau(u-\lambda)\,,\,\delta\lambda_\varphi\rangle_{\partial\mathcal{T}} \\
= \;& (\epsilon^{-1}\,\boldsymbol{q}\,,\,\boldsymbol{\delta q}_\varphi)_{\mathcal{T}} + \langle \boldsymbol{\delta q}_\varphi\cdot\boldsymbol{n}\,,\,\lambda - u\rangle_{\partial\mathcal{T}} + \langle \tau(u-\lambda)\,,\,\delta u_\varphi\rangle_{\partial\mathcal{T}}\,.
\end{aligned}
$$

Now, our aim is to bound each one of the three terms above. Applying Cauchy-Schwarz inequality and first approximation property in Lemma 3.6, we have

$$
(\epsilon^{-1}\boldsymbol{q}, \boldsymbol{\delta q}_\varphi)_K \le ||\epsilon^{-1/2}\boldsymbol{q}||_{[L^2(K)]^2}\,||\epsilon^{-1/2}\boldsymbol{\delta q}_\varphi||_{[L^2(K)]^2} \lesssim \csc(\beta_K)\,h_K||\epsilon^{-1/2}\boldsymbol{q}||^2_{[L^2(K)]^2}\,.
$$

On the other hand, since $\tau_K^{\boldsymbol{v}} \le \tau + \frac{1}{2}\boldsymbol{v}\cdot\boldsymbol{n}$ on ∂K, and taking into account second approximation property in Lemma 17, we derive

$$
\begin{aligned}
\langle \boldsymbol{\delta q}_\varphi\cdot\boldsymbol{n}\,,\,\lambda - u\rangle_{\partial K} &\le ||(\tau_K^{\boldsymbol{v}})^{-1/2}\boldsymbol{\delta q}_\varphi\cdot\boldsymbol{n}||_{L^2(\partial K)}\,||(\tau_K^{\boldsymbol{v}})^{1/2}(\lambda-u)||_{L^2(\partial K)} \\
&\le \left(\frac{\epsilon}{\tau_K^{\boldsymbol{v}}}\right)^{1/2} ||\epsilon^{-1/2}\boldsymbol{\delta q}_\varphi||_{L^2(\partial K)} \left\|\left(\tau + \frac{1}{2}\boldsymbol{v}\cdot\boldsymbol{n}\right)^{1/2}(\lambda-u)\right\|_{L^2(\partial K)} \\
&\lesssim \csc(\beta_K)\,h_K^{1/2}\left(\frac{\epsilon}{\tau_K^{\boldsymbol{v}}}\right)^{1/2} ||\epsilon^{-1/2}\boldsymbol{q}||_{[L^2(K)]^2} \left\|\left(\frac{h_K}{h_{\min,K}}\right)^{1/2}\left(\tau + \frac{1}{2}\boldsymbol{v}\cdot\boldsymbol{n}\right)^{1/2}(\lambda-u)\right\|_{L^2(\partial K)} \\
&\lesssim \csc(\beta_K)\,(h_K^2 + \epsilon\,h_K)^{1/2} \left\|\left(\frac{h_K}{h_{\min,K}}\right)^{1/2}\left(\tau + \frac{1}{2}\boldsymbol{v}\cdot\boldsymbol{n}\right)^{1/2}(\lambda-u)\right\|_{L^2(\partial K)} ||\epsilon^{-1/2}\boldsymbol{q}||_{[L^2(K)]^2}\,.
\end{aligned}
$$

In addition, considering **H.3**, it is not difficult to check

$$
\begin{aligned}
\langle \tau(u-\lambda)\,,\,\delta u_\varphi\rangle_{\partial K} &= \left\langle \left(\tau + \frac{1}{2}\boldsymbol{v}\cdot\boldsymbol{n}\right)(u-\lambda)\,,\,\delta u_\varphi\right\rangle_{\partial K} - \left\langle \frac{1}{2}(\boldsymbol{v}\cdot\boldsymbol{n})(u-\lambda)\,,\,\delta u_\varphi\right\rangle_{\partial K} \\
&\le \left(\left\|\left(\tau + \frac{1}{2}\boldsymbol{v}\cdot\boldsymbol{n}\right)^{1/2}(u-\lambda)\right\|_{L^2(\partial K)} + \left\|\left|\frac{1}{2}\boldsymbol{v}\cdot\boldsymbol{n}\right|^{1/2}(u-\lambda)\right\|_{L^2(\partial K)}\right) ||\delta u_\varphi||_{L^2(\partial K)} \\
&\lesssim \csc(\beta_K)\,h_K^{1/2}\left\|\left(\frac{h_K}{h_{\min,K}}\right)^{1/2}\left(\tau + \frac{1}{2}\boldsymbol{v}\cdot\boldsymbol{n}\right)^{1/2}(u-\lambda)\right\|_{L^2(\partial K)} ||u||_{L^2(K)}\,.
\end{aligned}
$$

Then, we have

$$B((\boldsymbol{q},u,\lambda),(\boldsymbol{\delta q}_\varphi,\delta u_\varphi,\delta\lambda_\varphi)) \lesssim \sum_{K\in\mathcal{T}} \csc(\beta_K)\, h_K\, ||\epsilon^{-1/2}\boldsymbol{q}||^2_{[L^2(K)]^2}$$
$$+ \sum_{K\in\mathcal{T}} \csc(\beta_K)\,(h_K^2 + \epsilon\, h_K)^{1/2} \left\| \left(\frac{h_K}{h_{\min,K}}\right)^{1/2} \left(\tau + \frac{1}{2}\boldsymbol{v}\cdot\boldsymbol{n}\right)^{1/2} (\lambda - u) \right\|_{L^2(\partial K)} ||\epsilon^{-1/2}\boldsymbol{q}||_{[L^2(K)]^2}$$
$$+ \sum_{K\in\mathcal{T}} \csc(\beta_K)\, h_K^{1/2} \left\| \left(\frac{h_K}{h_{\min,K}}\right)^{1/2} \left(\tau + \frac{1}{2}\boldsymbol{v}\cdot\boldsymbol{n}\right)^{1/2} (u - \lambda) \right\|_{L^2(\partial K)} ||u||_{L^2(K)}$$
$$\lesssim D_{\tilde{\beta}}\, h^{1/2}\, |||(\boldsymbol{q},u,\lambda)|||^2 .$$

Thanks to Lemma 3.1, we deduce there exists $\hat{C} > 0$ independent of the mesh size and ϵ such that

$$B((\boldsymbol{q},u,\lambda),(\boldsymbol{\delta q}_\varphi,\delta u_\varphi,\delta\lambda_\varphi)) \leq \hat{C}\, D_{\tilde{\beta}}\, h^{1/2}\, B((\boldsymbol{q},u,\lambda),(\boldsymbol{q}_\varphi,u_\varphi,\lambda_\varphi)) .$$

Then, we conclude that there exists $h_0 > 0$ such that for any $h < h_0$ there holds

$$B((\boldsymbol{q},u,\lambda),(\boldsymbol{\delta q}_\varphi,\delta u_\varphi,\delta\lambda_\varphi)) \leq \frac{1}{2}\, B((\boldsymbol{q},u,\lambda),(\boldsymbol{q}_\varphi,u_\varphi,\lambda_\varphi)) ,$$

from which is inferred that (applying again Lemma 3.1)

$$B((\boldsymbol{q},u,\lambda),(\Pi_{\boldsymbol{V}}\boldsymbol{q}_\varphi,\Pi_W u_\varphi,P_M\lambda_\varphi)) \geq \frac{1}{2}\, B((\boldsymbol{q},u,\lambda),(\boldsymbol{q}_\varphi,u_\varphi,\lambda_\varphi)) \geq \frac{C}{2}\, |||(\boldsymbol{q},u,\lambda)|||^2 .$$

Now, applying triangle inequality, Lemma 3.6, we also show that for any $h < h_0$, there holds

$$|||(\Pi_{\boldsymbol{V}}\boldsymbol{q}_\varphi,\Pi_W u_\varphi,P_M\lambda_\varphi)||| \lesssim D_{\tilde{\beta}}\, ||\varphi||_h\, |||(\boldsymbol{q},u,\lambda)||| ,$$

which let us to conclude the desired result. □

Now, we let $(\boldsymbol{q},u)$ be the exact solution, and $(\boldsymbol{q}_h,u_h,\widehat{u}_h) \in \boldsymbol{V}_h \times W_h \times M_h(0)$ the solution of (11). It is not difficult to check that (11) is consistent with the exact solution, which means

$$B((\boldsymbol{q},u,u),(\boldsymbol{r},w,\lambda)) = (f,w)_{\mathcal{T}} \quad \forall\, (\boldsymbol{r},w,\lambda) \in \boldsymbol{V}_h \times W_h \times M_h(0) .$$

This yields to the orthogonality relation

$$B((\boldsymbol{q}-\boldsymbol{q}_h,u-u_h,u-\widehat{u}_h),(\boldsymbol{r},w,\lambda)) = 0 \quad \forall\, (\boldsymbol{r},w,\lambda) \in \boldsymbol{V}_h \times W_h \times M_h(0) . \quad (23)$$

We introduce now

$$e_h^{\boldsymbol{q}} := \boldsymbol{q}_h - \Pi_{\boldsymbol{V}}\boldsymbol{q} \quad , \quad \boldsymbol{\delta q} := \boldsymbol{q} - \Pi_{\boldsymbol{V}}\boldsymbol{q}\,,$$

$$e_h^{u} := u_h - \Pi_{W}u \quad , \quad \delta u := u - \Pi_{W}u\,,$$

$$e_h^{\widehat{u}} := \widehat{u}_h - P_M u \quad , \quad \delta\widehat{u} := u - P_M u\,.$$

Thanks to (23) and definition of projections, we deduce the following identity

Lemma 3.8. *For any $(\boldsymbol{r}, w, \mu) \in \boldsymbol{V}_h \times W_h \times M_h(0)$, there holds*

$$\begin{aligned} B((e_h^{\boldsymbol{q}}, e_h^{u}, e_h^{\widehat{u}}), (\boldsymbol{r}, w, \mu)) \;&=\; (\epsilon^{-1}\,\boldsymbol{\delta q}, \boldsymbol{r})_{\mathcal{T}} + \langle \boldsymbol{\delta q}\cdot\boldsymbol{n}\,,\, w-\mu\rangle_{\partial\mathcal{T}} \\ &\quad + \langle(\tau + \boldsymbol{v}\cdot\boldsymbol{n})\delta u\,,\, w-\mu\rangle_{\partial\mathcal{T}} - \langle \tau\,\delta\widehat{u}\,,\, w-\mu\rangle_{\partial\mathcal{T}}\,. \end{aligned} \tag{24}$$

Finally, we can prove the main result of this paper. We recall that ∂^α and $\tilde{h}_K^\alpha$ have been introduced in (9).

Theorem 3.1. *For $h < h_0$ (introduced in Lemma 3.7), there exists $C > 0$, independent of mesh size and parameter ϵ, such that*

$$\frac{1}{||\varphi||_h}|||(\boldsymbol{q}-\boldsymbol{q}_h, u-u_h, u-\widehat{u}_h)||| \le C\,D_{\tilde{\beta}} \sum_{K\in\mathcal{T}} \left[\epsilon^{1/2} \sum_{|\alpha|=l_{\boldsymbol{q}}+1} \tilde{h}_K^{\alpha}\,||\partial^\alpha \nabla u||_{[L^2(K)]^2} \right.$$

$$\left. + \epsilon \sum_{\substack{|\alpha|=l_{\boldsymbol{q}}\\|\beta|=1}} \tilde{h}_K^{\alpha+0.5\beta}\,||\partial^{\alpha+\beta}\nabla u||_{[L^2(K)]^2} + \sum_{|\alpha|=l_{\boldsymbol{u}}+1} \tilde{h}_K^{\alpha}\,||\partial^\alpha u||_{L^2(K)} + \sum_{\substack{|\alpha|=l_u\\|\beta|=1}} \tilde{h}_K^{\alpha+0.5\beta}\,||\partial^{\alpha+\beta}u||_{L^2(K)} \right].$$

Proof. First, we bound each term on the right hand side in (24). We have, for each $K \in \mathcal{T}$

$$(\epsilon^{-1}\boldsymbol{\delta q}, \boldsymbol{r})_K \le ||\epsilon^{-1/2}\,\boldsymbol{\delta q}||_{[L^2(K)]^2}\,||\epsilon^{-1/2}\,\boldsymbol{r}||_{[L^2(K)]^2}\,.$$

$$
\begin{aligned}
\langle \boldsymbol{\delta q}\cdot\boldsymbol{n}\,,\, w-\mu\rangle_{\partial K} &= \langle (\tau_K^{\boldsymbol{v}})^{-1/2}\boldsymbol{\delta q}\cdot\boldsymbol{n}\,,\, (\tau_K^{\boldsymbol{v}})^{1/2}(w-\mu)\rangle_{\partial K} \\
&\leq \left(\frac{\epsilon}{\tau_K^{\boldsymbol{v}}}\right)^{1/2} ||\epsilon^{-1/2}\,\boldsymbol{\delta q}||_{[L^2(\partial K)]^2} \left\| \left(\tau + \frac{1}{2}\boldsymbol{v}\cdot\boldsymbol{n}\right)^{1/2} (w-\mu)\right\|_{L^2(\partial K)} \\
\langle (\tau + \boldsymbol{v}\cdot\boldsymbol{n})\,\delta u\,,\, w-\mu\rangle_{\partial K} &= \left\langle \left(\tau + \frac{1}{2}\boldsymbol{v}\cdot\boldsymbol{n}\right)\,\delta u\,,\, w-\mu\right\rangle_{\partial K} + \left\langle \frac{1}{2}(\boldsymbol{v}\cdot\boldsymbol{n})\,\delta u\,,\, w-\mu\right\rangle_{\partial K} \\
&\lesssim \left\| \left(\tau + \frac{1}{2}\boldsymbol{v}\cdot\boldsymbol{n}\right)^{1/2} (w-\mu)\right\|_{L^2(\partial K)} ||\delta u||_{L^2(\partial K)}\,,
\end{aligned}
$$

$$
\begin{aligned}
\langle \tau\,\delta\widehat{u}\,,\, w-\mu\rangle_{\partial K} &= \left\langle \left(\tau + \frac{1}{2}\boldsymbol{v}\cdot\boldsymbol{n}\right)\,\delta\widehat{u}\,,\, w-\mu\right\rangle_{\partial K} - \frac{1}{2}\,\langle (\boldsymbol{v}\cdot\boldsymbol{n})\,\delta\widehat{u}\,,\, w-\mu\rangle_{\partial K} \\
&\lesssim \left\| \left(\tau + \frac{1}{2}\boldsymbol{v}\cdot\boldsymbol{n}\right)^{1/2} (w-\mu)\right\|_{L^2(\partial K)} ||\delta\widehat{u}||_{L^2(\partial K)}\,.
\end{aligned}
$$

Next, we take into account the approximation results (Lemmas 3.5 and 3.4)

$$
\begin{aligned}
||\epsilon^{-1/2}\boldsymbol{\delta q}||_{[L^2(K)]^2} &\lesssim \epsilon^{-1/2}\,\csc(\beta_K) \sum_{|\alpha|=l_{\boldsymbol{q}}+1} \tilde{h}_K^{\alpha}\,||\partial^{\alpha}\boldsymbol{q}||_{[L^2(K)]^2}\,, \\
||\epsilon^{-1/2}\boldsymbol{\delta q}||_{[L^2(\partial K)]^2} &\lesssim \epsilon^{-1/2}\,\csc(\beta_K)\left(\frac{h_K}{h_{\min,K}}\right)^{1/2} \sum_{\substack{|\alpha|=l_{\boldsymbol{q}} \\ |\beta|=1}} \tilde{h}_K^{\alpha+0.5\beta}\,||\partial^{\alpha+\beta}\boldsymbol{q}||_{[L^2(K)]^2}\,, \\
||\delta u||_{L^2(\partial K)} &\lesssim \csc(\beta_K)\left(\frac{h_K}{h_{\min,K}}\right)^{1/2} \sum_{\substack{|\alpha|=l_u \\ |\beta|=1}} \tilde{h}_K^{\alpha+0.5\beta}\,||\partial^{\alpha+\beta}u||_{L^2(K)}\,, \\
||\delta\widehat{u}||_{L^2(\partial K)} &\lesssim \csc(\beta_K)\left(\frac{h_K}{h_{\min,K}}\right)^{1/2} \sum_{\substack{|\alpha|=l_u \\ |\beta|=1}} \tilde{h}_K^{\alpha+0.5\beta}\,||\partial^{\alpha+\beta}u||_{L^2(K)}\,,
\end{aligned}
$$

where $l_{\boldsymbol{q}}\,,\, l_u \in [0,k]$, and C a positive constant that does not depend on the maximum angle β_K. Then, for any $(\boldsymbol{r}, w, \mu) \in \boldsymbol{V}_h \times W_h \times M_h(0)$, we deduce

$$B((e_h^{\boldsymbol{q}}, e_h^u, e_h^{\widehat{u}}), (\boldsymbol{r}, w, \mu)) \lesssim \sum_{K\in\mathcal{T}} \csc(\beta_K) \left[\sum_{\substack{|\alpha|=l_{\boldsymbol{q}} \\ |\beta|=1}} \tilde{h}_K^{\alpha+0.5\beta} \, ||\partial^{\alpha+\beta}\boldsymbol{q}||_{[L^2(K)]^2} \right.$$

$$\left. + \epsilon^{-1/2} \sum_{|\alpha|=l_{\boldsymbol{q}}+1} \tilde{h}_K^{\alpha} \, ||\partial^{\alpha}\boldsymbol{q}||_{[L^2(K)]^2} + \sum_{\substack{|\alpha|=l_u \\ |\beta|=1}} \tilde{h}_K^{\alpha+0.5\beta} \, ||\partial^{\alpha+\beta}u||_{L^2(K)} \right] |||(\boldsymbol{r}, w, \mu)||| \, .$$

Since $(e_h^{\boldsymbol{q}}, e_h^u, e_h^{\widehat{u}}) \in \boldsymbol{V}_h \times W_h \times M_h(0)$, we apply Lemma 3.7, and then for h small enough we have

$$\frac{1}{||\varphi||_h} |||(e_h^{\boldsymbol{q}}, e_h^u, e_h^{\widehat{u}})||| \lesssim D_{\tilde{\beta}} \sum_{K\in\mathcal{T}} \left[\sum_{\substack{|\alpha|=l_{\boldsymbol{q}} \\ |\beta|=1}} \tilde{h}_K^{\alpha+0.5\beta} \, ||\partial^{\alpha+\beta}\boldsymbol{q}||_{[L^2(K)]^2} \right.$$

$$\left. + \epsilon^{-1/2} \sum_{|\alpha|=l_{\boldsymbol{q}}+1} \tilde{h}_K^{\alpha} \, ||\partial^{\alpha}\boldsymbol{q}||_{[L^2(K)]^2} + \sum_{\substack{|\alpha|=l_u \\ |\beta|=1}} \tilde{h}_K^{\alpha+0.5\beta} \, ||\partial^{\alpha+\beta}u||_{L^2(K)} \right] . \tag{25}$$

As $\boldsymbol{q} = \epsilon \nabla u$, we derive

$$\frac{1}{||\varphi||_h} |||(e_h^{\boldsymbol{q}}, e_h^u, e_h^{\widehat{u}})||| \lesssim D_{\tilde{\beta}} \sum_{K\in\mathcal{T}} \left[\epsilon \sum_{\substack{|\alpha|=l_{\boldsymbol{q}} \\ |\beta|=1}} \tilde{h}_K^{\alpha+0.5\beta} \, ||\partial^{\alpha+\beta}\nabla u||_{[L^2(K)]^2} \right.$$

$$\left. + \epsilon^{1/2} \sum_{|\alpha|=l_{\boldsymbol{q}}+1} \tilde{h}_K^{\alpha} \, ||\partial^{\alpha}\nabla u||_{[L^2(K)]^2} + \sum_{\substack{|\alpha|=l_u \\ |\beta|=1}} \tilde{h}_K^{\alpha+0.5\beta} \, ||\partial^{\alpha+\beta}u||_{L^2(K)} \right] .$$

By approximation properties of the projection, we also deduce

$$\frac{1}{||\varphi||_h} |||(\boldsymbol{\delta q}, \delta u, \delta\widehat{u})||| \lesssim D_{\tilde{\beta}} \sum_{K\in\mathcal{T}} \left[\epsilon^{1/2} \sum_{|\alpha|=l_{\boldsymbol{q}}+1} \tilde{h}_K^{\alpha} \, ||\partial^{\alpha}\nabla u||_{[L^2(K)]^2} \right.$$

$$\left. + \sum_{|\alpha|=l_{\boldsymbol{u}}+1} \tilde{h}_K^{\alpha} \, ||\partial^{\alpha}u||_{L^2(K)} + \sum_{\substack{|\alpha|=l_u \\ |\beta|=1}} \tilde{h}_K^{\alpha+0.5\beta} \, ||\partial^{\alpha+\beta}u||_{L^2(K)} \right] .$$

Finally, applying triangle inequality, we derive the result and conclude the proof.

□

Remark 3.1. *When, in addition,* $\epsilon \lesssim h_{\min,K} \quad \forall\, K \in \mathcal{T}$*, and the regularity of* u *and* $\boldsymbol{q}$ *are such that* $l_u = k$ *and* $l_{\boldsymbol{q}} = \max\{0, k-1\}$ *respectively, we obtain*

$$\frac{1}{||\varphi||_h} |||(\boldsymbol{q} - \boldsymbol{q}_h, u - u_h, u - \widehat{u}_h)||| = \mathcal{O}(h^{k+0.5}) .$$

Otherwise, the above expression would behave as $\mathcal{O}(h^r)$*, with* $r \in [k - 1/2, k + 1/2]$*, and makes sense for* $k > 0$*.*

Remark 3.2. *The current analysis requires the maximum angle condition, which allows us to bound* $D_{\tilde{\beta}}$ *uniformly in our main a priori result (cf Theorem 3.1). Otherwise, this constant* $D_{\tilde{\beta}}$ *could blow up as the maximum angle is closer to* π*.*

Remark 3.3. *In order to obtain an error estimate of* $\boldsymbol{\sigma} - \boldsymbol{\sigma}_h$*, we take into account the local inequality*

$$\begin{aligned} ||\boldsymbol{\sigma} - \boldsymbol{\sigma}_h||_{[L^2(K)]^2} \quad \leq \quad & \epsilon^{1/2} \, ||\epsilon^{-1/2}(\boldsymbol{q} - \boldsymbol{q}_h)||_{[L^2(K)]^2} + ||\boldsymbol{v}||_{[L^\infty(K)]^2} \, ||u - u_h||_{L^2(K)} \\ & + \sum_{|\alpha| = l_r + 1} \tilde{h}_K^{\alpha} ||\partial^\alpha (u\, \boldsymbol{v})||_{[L^2(K)]^2} \quad \forall\, K \in \mathcal{T} . \end{aligned}$$

Remark 3.4. *Our main result, given in Theorem 3.1, is valid also when we consider the numerical flux introduced in [19]*

$$\widehat{\boldsymbol{\sigma}}_h := \boldsymbol{q}_h + \widehat{u}_h \, \boldsymbol{v} + \tau(u_h - \widehat{u}_h) \quad \text{ on } \partial\mathcal{T} .$$

In this case, we need to assume that the parameter τ *is defined such that* $\tau - \frac{1}{2}\boldsymbol{v}\cdot\boldsymbol{n} > 0$ *on* $\partial\mathcal{T}$*. This should be taken into account to define the corresponding norms, the analogous properties* ***H.1-H.3*** *for* τ*, etc.*

4. Numerical results

In the following examples the stabilization parameter τ in each edge e is taken as $\tau^e = \tau_d^e + \tau_c^e$, where $\tau_c^e := \sup_{\boldsymbol{x}\in e} |\boldsymbol{v}(\boldsymbol{x}) \cdot \boldsymbol{n}|$ and $\tau_d^e := \min(\epsilon/h_e, 1)$. We compute the errors $e_{\boldsymbol{q}} := \|\epsilon^{-1/2}(\boldsymbol{q} - \boldsymbol{q}_h)\|_{[L^2(\Omega)]^2}$, $e_u := \|u - u_h\|_{L^2(\Omega)}$, $e_{\boldsymbol{\sigma}} := \|\boldsymbol{\sigma} - \boldsymbol{\sigma}_h\|_{[L^2(\Omega)]^2}$,

$$e_{\hat{u}} : \quad = \quad \left(\sum_{K\in\mathcal{T}} \left\| \left(\frac{h_K}{h_{\min,K}} \right)^{1/2} \left(\tau + \frac{1}{2}\boldsymbol{v}\cdot\boldsymbol{n} \right)^{1/2} (u_h - \widehat{u}_h) \right\|^2_{L^2(\partial K)} \right)^{1/2} .$$

On the other hand, the estimate provided in Theorem 3.1 depends on $\|\varphi\|_h$, which depends on the triangulation $\mathcal{T}$ and verifies

$$\chi \max_{K\in\mathcal{T}}\left(\frac{h_K}{h_{\min,K}}\right) \leq \|\varphi\|_h \leq \|\mathrm{e}^{-\psi}\|_{W^{k+1,\infty}(\Omega)} + \chi \max_{K\in\mathcal{T}}\left(\frac{h_K}{h_{\min,K}}\right).$$

Since χ and $\|\mathrm{e}^{-\psi}\|_{W^{k+1,\infty}(\Omega)}$ are independent of the mesh, the quantity $M_{\mathcal{T}} := \max_{K\in\mathcal{T}}\left(\frac{h_K}{h_{\min,K}}\right)$ is a suitable indicator of the behavior of $\|\varphi\|_h$. Based on this observation, for each variable, we compute the experimental order of convergence (e.o.c.) as

$$\text{e.o.c.} = \log\left(\frac{e_{\mathcal{T}_1}/M_{\mathcal{T}_1}}{e_{\mathcal{T}_2}/M_{\mathcal{T}_2}}\right)\Big/ \log(h_{\mathcal{T}_1}/h_{\mathcal{T}_2}),$$

where $e_{\mathcal{T}_1}$ and $e_{\mathcal{T}_2}$ are the errors associated to the corresponding variable considering two consecutive meshsizes $h_{\mathcal{T}_1}$ and $h_{\mathcal{T}_2}$, respectively.

4.1. Unstructured meshes

In this section we show the results obtained using anisotropic unstructured meshes. We use BAMG ([30]) to generate an initial anisotropic mesh. Since the goal of this work is to show the performance of the HDG method, in all the example the exact solution is known. Hence, BAMG creates the mesh based on a metric tensor that involves the Hessian of the solution. Then, we uniformly refine this initial mesh by dividing the triangles by the midpoints of the edges. This procedure keeps the anisotropy of the mesh, preserves angles and $M_{\mathcal{T}}$ is the same for every mesh.

4.1.1. Boundary layers

Example 1. We consider the domain $\Omega =]0,1[^2$ and velocity $\boldsymbol{v} = (1,1)^t$. The exact solution is taken to be $u(x,y) = xy\dfrac{(1-\mathrm{e}^{\epsilon^{-1}(x-1)})(1-\mathrm{e}^{\epsilon^{-1}(y-1)})}{(1-\mathrm{e}^{-\epsilon^{-1}})(1-\mathrm{e}^{-\epsilon^{-1}})} - \sin(3x\pi/2) - \sin(3y\pi/2) + 2$. It has boundary layers at $\{x=1\}$ and $\{y=1\}$ for small values of ϵ. Here, we have added sinusoidal terms so that, away from the boundary layers, the solution does not behave as a quadratic function when ϵ is small. This will allows us to study the convergence rates for $k > 1$. In this

first example we set $\epsilon = 10^{-3}$. In Figure 1 we show the initial mesh and a zoom of it at the top-right corner. Figure 2 displays the approximate solution u_h for $k = 1$ and $k = 2$ considering a uniform mesh (left) and the anisotropic mesh (right) showed in Figure 1. We clearly observe that the uniform mesh does not resolve the boundary layer, but if that suitable anisotropic mesh is considered, the approximation does not exhibit oscillations near the layers. In this case, all the meshes satisfy $\max_{K\in\mathcal{T}} \left(\frac{h_K}{h_{\min,K}}\right)^{1/2} = 7.14$ and $\max_{K\in\mathcal{T}} \beta_K = 179.5394^\circ$. Table 1 shows the history of convergence of the method which agrees with Remark 3.1 since the solution is smooth and $\max_{K\in\mathcal{T}} \left(\frac{h_K}{h_{\min,K}}\right)^{1/2}$ is bounded. In some cases ($k = 0$, 1 and 2) the order of convergence of u is higher than expected. We point out that since the maximum angle of these meshes is close to π, the constant $D_{\tilde{\beta}}$ in Theorem 3.1 is big. Even though, errors in Table 1 are small.

On the other hand, we numerically study the spectral condition number κ of the global matrix associated to $\widehat{u}_h$. We recall that, for pure diffusion problems, [31] reported numerical experiments indicating that κ is proportional to $(k+1)h^{-2}$. For the case of convection-dominated diffusion problems, [15] proved that κ behaves as h^{-2} on isotropic meshes. In Table 2 we display the experimental order (e.o.) such that κ is proportional to $h^{(\text{e.o.})}$. We observe that it is close to -2, which agrees with the results presented in [15, 31].

Example 2. We consider the same squared domain as previous example and the exact solution

$$u(x,y) = x^2\big(y(1-y) + \mathrm{e}^{-\frac{y}{\sqrt{\epsilon}}} + \mathrm{e}^{-\frac{(1-y)}{\sqrt{\epsilon}}}\big),$$

with $\epsilon = 10^{-3}$. We take $\boldsymbol{v} = (1,0)^t$. This solution has two boundary layer on the horizontal axis. The initial mesh is displayed in Figure 3 (left) and u_h considering $k = 1$ and $N = 7824$ is shown on the right. The history of convergence of the method provides similar conclusions as in previous example, hence we omit the corresponding table. Here, all the meshes satisfy $\max_{K\in\mathcal{T}} \left(\frac{h_K}{h_{\min,K}}\right)^{1/2} = 17.87$ and $\max_{K\in\mathcal{T}} \beta_K = 179.6203^\circ$.

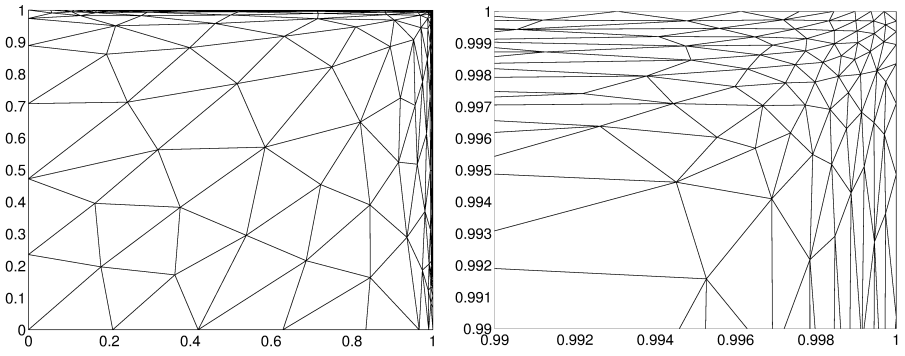

Figure 1: Example 1: Initial mesh with $N = 823$ (left) and a zoom-in on the upper-right corner (right).

4.1.2. Interior layer

Example 3. Let us consider the same domain as before and the exact solution

$$u(x,y) = \frac{1}{1+\mathrm{e}^{\frac{-(x+y-0.8)}{5\epsilon}}}$$

with $\epsilon = 10^{-3}$. It has an interior layer along the segment described by $x + y = 0.8$. We take $\boldsymbol{v} = (2,3)^t$. In Figure 4 (left) we display the initial mesh generated with BAMG. Its corresponding approximated solution u_h ($k = 1$) is depicted on the right. No oscillation are observed near the interior layer since the initial mesh is fine enough in that region. In this case, all the meshes satisfy $\max_{K\in\mathcal{T}} \left(\frac{h_K}{h_{\min,K}}\right)^{1/2} = 18.27$ and $\max_{K\in\mathcal{T}} \beta_K = 179.7651°$. Once again, in accordance with Remark 3.1, the order of convergence for $e_{\boldsymbol{q}}$ and $e_{\widehat{u}}$ seems to be at least $h^{k+0.5}$. Moreover, for $k = 0$, 1 and 2 the order of convergence for e_u is higher than expected.

4.1.3. Non constant convection

Example 4. We consider the same exact solution as in Example 3 but considering a non-constant convective field $\boldsymbol{v} = (u,u)^t$. We do not displays the results since they provide similar conclusion to the ones obtained in Example 3.

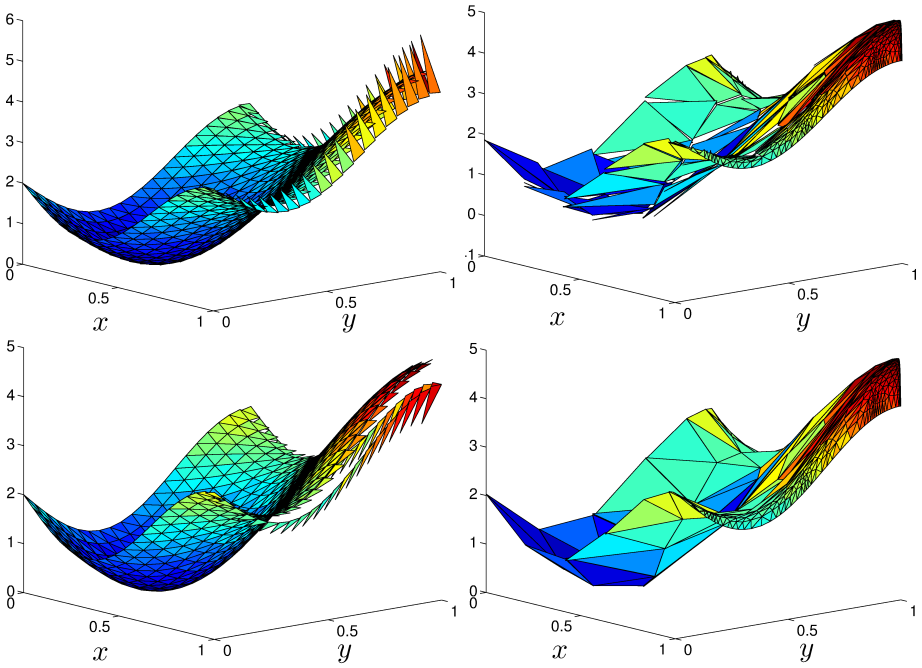

Figure 2: Approximate solution u_h of Example 1 considering $k = 1$ (top row) and $k = 2$ (bottom row) when $\epsilon = 10^{-3}$. Left column: uniform mesh with $N = 882$ elements. Top-left: anisotropic mesh $N = 823$ elements.

4.2. Shishkin meshes

Example 5. We choose the same problem as in Example 1, but considering a Shishkin mesh (Figure 5) constructed as follows (we refer to Section 2.4.2 in [32]). We set $a = \min\{0.5, (k+1)\epsilon \log(M)\}$, for a given an integer M. Then, the intervals $[0, 1-a]$ and $[1-a, 1]$ (on both axes) are uniformly divided in M subintervals. Finally, each rectangle on this grid is divided in two triangles with hypotenuse parallel to the vector $\boldsymbol{v} = (1,1)^t$. Because of this construction, $\max_{K\in\mathcal{T}} \beta_K = 90^\circ$ and then $D_{\tilde{\beta}} = 1$. Moreover, $M_{\mathcal{T}}$ decreases with k and h as we can deduce from Table 4. Moreover, ϵ is always greater than $h_{min,K}$ for all K in the triangulation $\mathcal{T}$. Hence, Remark 3.1 predicts an order of convergence of h^r with $r \in [k - 1/2, k + 1/2]$.

k	N	$e_{\boldsymbol{q}}$	e.o.c	e_u	e.o.c	$e_{\boldsymbol{\sigma}}$	e.o.c	$e_{\widehat{u}}$	e.o.c
0	823	2.81e-01	$--$	2.72e-01	$--$	3.85e-01	$--$	1.92e+00	$--$
	3292	1.87e-01	0.59	1.38e-01	0.98	1.95e-01	0.98	1.39e+00	0.46
	13168	1.25e-01	0.58	7.07e-02	0.96	1.00e-01	0.96	1.02e+00	0.45
	52672	8.62e-02	0.54	3.71e-02	0.93	5.24e-02	0.93	7.50e-01	0.44
	210688	6.06e-02	0.51	2.02e-02	0.88	2.85e-02	0.88	5.59e-01	0.42
1	823	3.30e-02	$-$	2.44e-02	$--$	3.45e-02	$--$	2.26e-01	$--$
	3292	1.05e-02	1.66	5.86e-03	2.06	8.28e-03	2.06	8.45e-02	1.42
	13168	4.03e-03	1.38	1.39e-03	2.08	1.95e-03	2.09	3.10e-02	1.45
	52672	1.61e-03	1.32	3.22e-04	2.10	4.48e-04	2.12	1.12e-02	1.47
	210688	6.61e-04	1.29	7.25e-05	2.15	9.68e-05	2.21	4.08e-03	1.46
2	823	4.85e-03	$--$	1.90e-03	$--$	2.68e-03	$--$	2.66e-02	$--$
	3292	9.84e-04	2.30	2.21e-04	3.10	3.16e-04	3.09	5.82e-03	2.19
	13168	1.61e-04	2.61	2.60e-05	3.09	3.74e-05	3.08	1.28e-03	2.19
	52672	3.05e-05	2.40	3.03e-06	3.10	4.37e-06	3.10	2.63e-04	2.28
	210688	6.20e-06	2.30	3.55e-07	3.10	4.98e-07	3.13	5.21e-05	2.34
3	823	1.37e-03	$--$	1.57e-04	$--$	2.28e-04	$--$	4.42e-03	$--$
	3292	2.18e-04	2.66	1.13e-05	3.79	2.05e-05	3.48	8.59e-04	2.36
	13168	2.18e-05	3.32	9.29e-07	3.61	1.91e-06	3.43	1.26e-04	2.77
	52672	2.03e-06	3.42	8.39e-08	3.47	1.87e-07	3.35	1.51e-05	3.06
	210688	1.30e-07	3.97	7.09e-09	3.56	1.51e-08	3.63	1.64e-06	3.20

Table 1: History of convergence of Example 1.

In Table 5 we display the history of convergence of the method considering $\epsilon = 10^{-3}$. First of all, when $k = 0$, we observe no convergence for $\boldsymbol{q}_h$ which agrees with Remark 3.1 because it does not guarantee convergence for this case. Even though the error $e_{\boldsymbol{q}}$ decreases when N increases, $M_{\mathcal{T}}$ decreases faster for $N \geq 2048$ which explains the negative value for the *e.o.c*. The experimental convergence rate for e_u and $e_{\widehat{u}}$ seems to behave as expected, i.e., $\mathcal{O}(h^r)$ with

	$k=1$		$k=2$		$k=3$	
N	κ	e.o.	κ	e.o.	κ	e.o.
823	7.18e+04	–	1.17e+05	–	2.00e+05	–
3292	4.45e+05	−2.63	7.21e+05	−2.62	1.16e+06	−2.53
13168	1.70e+06	−1.94	2.74e+06	−1.93	4.42e+06	−1.93
52672	6.64e+06	−1.97	1.07e+07	−1.96	1.72e+07	−1.96
210688	2.62e+07	−1.98	4.23e+07	−1.98	6.81e+07	−1.98

Table 2: Condition number (κ) of the global matrix of Example 1.

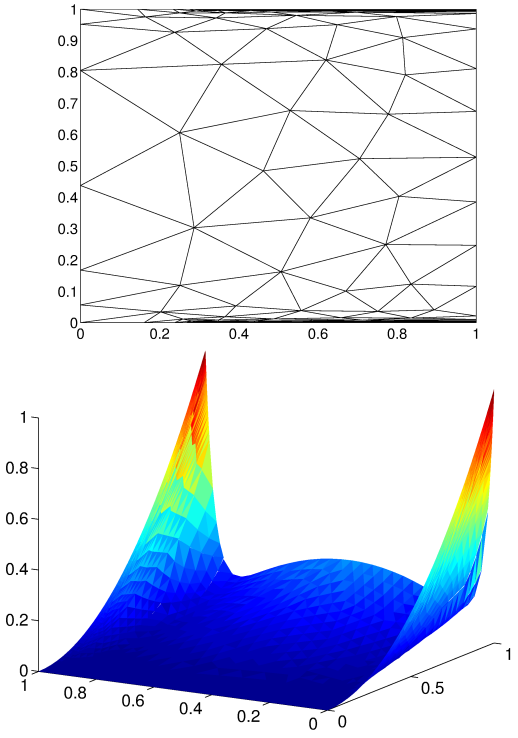

Figure 3: Example 2: Initial mesh with $N = 489$ (left). Approximate solution u_h with $N = 7824$, $k = 1$ and $\epsilon = 10^{-3}$ (right).

$r \geq 0.5$. On the other hand, when $k > 0$, all the variables converge with order in the range predicted by Remark 3.1. Except that, the convergence rate for e_u

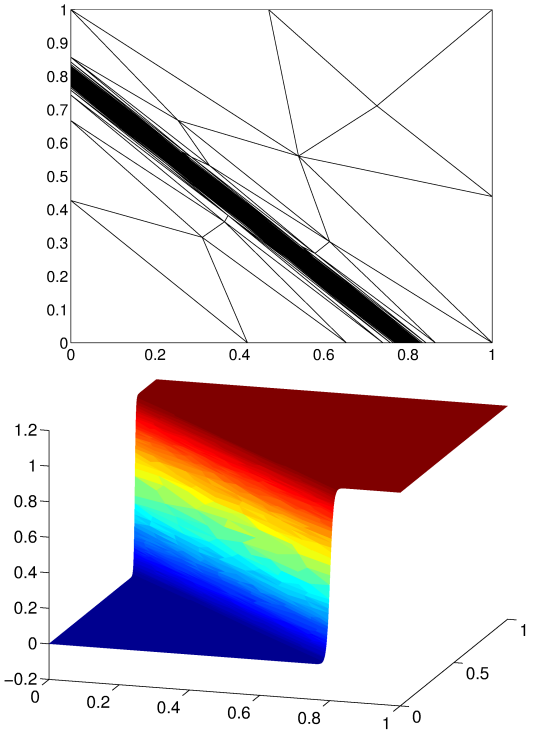

Figure 4: Example 3: Initial mesh with $N = 1020$ (left) and corresponding approximated solution u_h $(k = 1)$.

is a bit higher than expected when $k = 1$.

We consider now $\epsilon = 10^{-9}$. As we see in Table 6, $M_{\mathcal{T}}$ is higher than the one corresponding to previous case but also decreases with N and k. According to Table 7, the experimental rate of convergence of all the variables agrees with the range predicted by Remark 3.1. Once again, u_h converges to u with an order a bit higher than $h^{k+0.5}$. The error $e_{\boldsymbol{q}}$ in the last mesh and $k = 3$ is probably being affected by round-off errors. In fact, $e_{\boldsymbol{q}}$ has been weighted by $\epsilon^{-1/2}$ which in this case is $10^{4.5}$, i.e., without this weight the error would be of order 10^{-12}.

k	N	$e_{\boldsymbol{q}}$	e.o.c	e_u	e.o.c	$e_{\boldsymbol{\sigma}}$	e.o.c	$e_{\widehat{u}}$	e.o.c
0	1020	7.02e-04	−−	9.46e-04	−−	3.41e-03	−−	7.69e-01	−−
	4080	4.72e-04	0.57	4.87e-04	0.96	1.75e-03	0.96	5.45e-01	0.50
	16320	3.75e-04	0.33	2.60e-04	0.91	9.35e-04	0.91	3.86e-01	0.50
	65280	3.42e-04	0.13	1.41e-04	0.88	5.08e-04	0.88	2.74e-01	0.49
	261120	3.28e-04	0.06	8.14e-05	0.80	2.93e-04	0.80	1.96e-01	0.49
1	1020	4.27e-05	−−	2.05e-05	−−	7.40e-05	−−	8.11e-03	−−
	4080	1.37e-05	1.64	3.91e-06	2.39	1.41e-05	2.39	2.89e-03	1.49
	16320	4.05e-06	1.76	5.95e-07	2.72	2.16e-06	2.71	1.03e-03	1.49
	65280	1.19e-06	1.77	1.20e-07	2.31	4.35e-07	2.31	3.65e-04	1.49
	261120	3.92e-07	1.60	3.08e-08	1.96	1.11e-07	1.97	1.30e-04	1.49
2	1020	5.61e-06	−−	4.45e-06	−−	1.60e-05	−−	3.29e-04	−−
	4080	1.71e-06	1.72	3.76e-07	3.57	1.34e-06	3.58	7.11e-05	2.21
	16320	4.32e-07	1.98	4.68e-08	3.01	1.55e-07	3.11	1.57e-05	2.18
	65280	6.75e-08	2.68	5.40e-09	3.12	1.58e-08	3.30	3.28e-06	2.26
	261120	9.51e-09	2.83	5.32e-10	3.34	2.54e-09	2.64	6.23e-07	2.40
3	1020	2.65e-06	−−	1.09e-06	−−	3.92e-06	−−	4.35e-05	−−
	4080	7.85e-07	1.76	8.76e-08	3.63	2.97e-07	3.72	1.01e-05	2.11
	16320	1.19e-07	2.72	1.26e-08	2.80	4.12e-08	2.85	2.07e-06	2.28
	65280	1.10e-08	3.44	1.12e-09	3.49	3.52e-09	3.55	2.76e-07	2.90
	261120	7.13e-10	3.94	7.13e-11	3.97	2.10e-10	4.07	2.82e-08	3.29

Table 3: History of convergence of Example 3.

5. Conclusions and final comments

In this work we have developed an a priori error analysis for the convection dominated diffusion problem in 2D, when using the HDG method on a family of anisotropic triangulations. We adapt ideas given in [12] and [19], in order to follow the dependence of the constants on the diffusion coefficient ϵ, and in this case also on the uniform bound of the maximum angle of the triangulation.

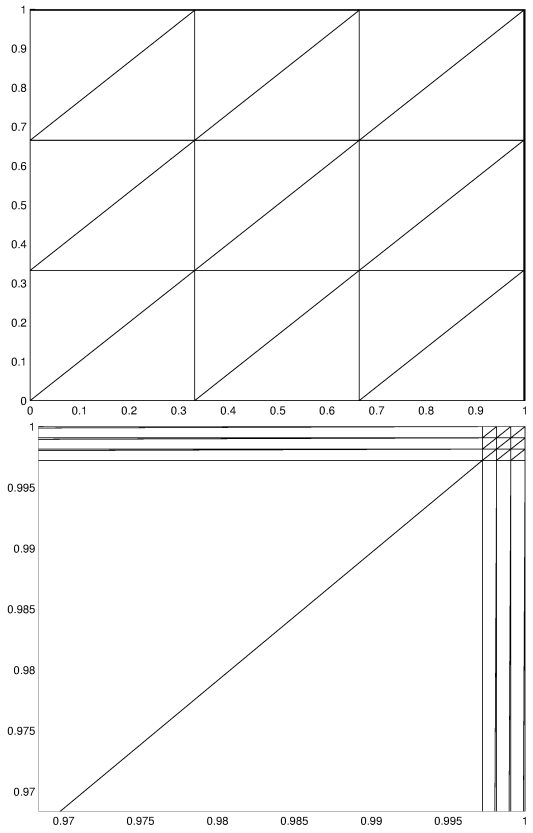

Figure 5: Shishkin mesh for example 1 with $M = 3$, $k = 1$ and $\epsilon = 10^{-3}$ (left) and a zoom on the upper right corner (right).

As result, we deduce that when ϵ is small enough, the corresponding rate of convergence is $\mathcal{O}(h^{k+0.5})$. Otherwise, the rate of convergence would behave as $\mathcal{O}(h^r)$, for some $r \in [k - 0.5, k + 0.5]$. Numerical examples are in agreement with our theoretical results, even when the maximum angle on the family of triangulations is very close to π. Since the a priori error analysis require usual L^2-projectors and does not need the use of Lagrange interpolation operator, we believe that the analysis can be adapted for 3D case (anisotropic tetrahedra) in a natural way. On the other hand, as the presence of boundary or inner layers is very natural in this kind of problems, it would be better to count with

N	$k=0$	$k=1$	$k=2$	$k=3$
32	3.78e+01	2.68e+01	2.19e+01	1.90e+01
128	2.68e+01	1.90e+01	1.55e+01	1.34e+01
512	2.19e+01	1.55e+01	1.26e+01	1.09e+01
2048	1.90e+01	1.34e+01	1.09e+01	9.44e+00
8192	1.70e+01	1.20e+01	9.76e+00	8.43e+00
32768	1.55e+01	1.09e+01	8.90e+00	7.69e+00
131072	1.43e+01	1.01e+01	8.23e+00	7.11e+00

Table 4: $\max_K \left(\frac{h_K}{h_{\min,K}}\right)^{1/2}$ for meshes of Example 5 with $\epsilon = 10^{-3}$.

an a posteriori error estimator for anisotropic meshes. In this way, an adaptive refinement could perform, with the aim of recognize the region of the domain where the layers are, improving the quality of approximation in the process. These are the subjects of ongoing work.

Acknowledgments

First author has been partially supported by CONICYT FONDECYT 1130158 and project AFB170001 of the PIA Program: Concurso Apoyo a Centros Científicos y Tecnológicos de Excelencia con Financiamiento Basal, by project VRID-Enlace No. 218.013.044-1.0, Universidad de Concepción, and by Centro de Investigación en Ingeniería Matemática (CI^{2}MA), Universidad de Concepción. Second author has been partially supported by CONICET-Argentina under grant PID No. 14420140100027CO, by ANPCyT PICT No. 2014-1771, and by Universidad de Buenos Aires under grant UBACyT No. 20020120100050. Finally, third author has been partially supported by CONICYT FONDECYT 1160320 and project AFB170001 of the PIA Program: Concurso Apoyo a Centros Científicos y Tecnológicos de Excelencia con Financiamiento Basal, and by Centro de Investigación en Ingeniería Matemática (CI^{2}MA), Universidad de Concepción.

References

[1] B. Cockburn, Discontinuous Galerkin methods for convection-dominated problems, in: High-order methods for computational physics, Vol. 9 of Lect. Notes Comput. Sci. Eng., Springer, Berlin, 1999, pp. 69–224. doi:10.1007/978-3-662-03882-6_2.
URL https://doi.org/10.1007/978-3-662-03882-6_2

[2] B. Cockburn, C.-W. Shu, Runge-Kutta discontinuous Galerkin methods for convection-dominated problems, J. Sci. Comput. 16 (3) (2001) 173–261. doi:10.1023/A:1012873910884.
URL https://doi.org/10.1023/A:1012873910884

[3] P. Castillo, B. Cockburn, D. Schötzau, C. Schwab, Optimal a priori error estimates for the *hp*-version of the local discontinuous Galerkin method for convection-diffusion problems, Math. Comp. 71 (238) (2002) 455–478. doi:10.1090/S0025-5718-01-01317-5.
URL https://doi.org/10.1090/S0025-5718-01-01317-5

[4] B. Cockburn, C. Dawson, Some extensions of the local discontinuous Galerkin method for convection-diffusion equations in multidimensions, in: The mathematics of finite elements and applications, X, MAFELAP 1999 (Uxbridge), Elsevier, Oxford, 2000, pp. 225–238. doi:10.1016/B978-008043568-8/50014-6.
URL https://doi.org/10.1016/B978-008043568-8/50014-6

[5] B. Cockburn, B. Dong, J. Guzmán, A superconvergent LDG-hybridizable Galerkin method for second-order elliptic problems, Math. Comp. 77 (264) (2008) 1887–1916. doi:10.1090/S0025-5718-08-02123-6.
URL https://doi.org/10.1090/S0025-5718-08-02123-6

[6] B. Cockburn, C.-W. Shu, The local discontinuous Galerkin method for time-dependent convection-diffusion systems, SIAM J. Numer. Anal. 35 (6) (1998) 2440–2463. doi:10.1137/S0036142997316712.
URL https://doi.org/10.1137/S0036142997316712

[7] P. Houston, C. Schwab, E. Süli, Discontinuous *hp*-finite element methods for advection-diffusion-reaction problems, SIAM J. Numer. Anal. 39 (6) (2002) 2133–2163. doi:10.1137/S0036142900374111.
URL https://doi.org/10.1137/S0036142900374111

[8] B. Cockburn, B. Dong, An analysis of the minimal dissipation local discontinuous Galerkin method for convection-diffusion problems, J. Sci. Comput. 32 (2) (2007) 233–262. doi:10.1007/s10915-007-9130-3.
URL https://doi.org/10.1007/s10915-007-9130-3

[9] P. Bochev, T. J. R. Hughes, G. Scovazzi, A multiscale discontinuous Galerkin method, in: Large-scale scientific computing, Vol. 3743 of Lecture Notes in Comput. Sci., Springer, Berlin, 2006, pp. 84–93. doi:10.1007/11666806_8.
URL https://doi.org/10.1007/11666806_8

[10] A. Buffa, T. J. R. Hughes, G. Sangalli, Analysis of a multiscale discontinuous Galerkin method for convection-diffusion problems, SIAM J. Numer. Anal. 44 (4) (2006) 1420–1440. doi:10.1137/050640382.
URL https://doi.org/10.1137/050640382

[11] T. J. R. Hughes, G. Scovazzi, P. B. Bochev, A. Buffa, A multiscale discontinuous Galerkin method with the computational structure of a continuous Galerkin method, Comput. Methods Appl. Mech. Engrg. 195 (19-22) (2006) 2761–2787. doi:10.1016/j.cma.2005.06.006.
URL https://doi.org/10.1016/j.cma.2005.06.006

[12] B. Ayuso, L. D. Marini, Discontinuous Galerkin methods for advection-diffusion-reaction problems, SIAM J. Numer. Anal. 47 (2) (2009) 1391–1420. doi:10.1137/080719583.
URL https://doi.org/10.1137/080719583

[13] H. Zarin, H.-G. Roos, Interior penalty discontinuous approximations of convection-diffusion problems with parabolic layers, Numer. Math. 100 (4)

(2005) 735–759. doi:10.1007/s00211-005-0598-1.
URL https://doi.org/10.1007/s00211-005-0598-1

[14] C. E. Baumann, J. T. Oden, A discontinuous *hp* finite element method for convection-diffusion problems, Comput. Methods Appl. Mech. Engrg. 175 (3-4) (1999) 311–341. doi:10.1016/S0045-7825(98)00359-4.
URL https://doi.org/10.1016/S0045-7825(98)00359-4

[15] H. Egger, J. Schöberl, A hybrid mixed discontinuous Galerkin finite-element method for convection-diffusion problems, IMA J. Numer. Anal. 30 (4) (2010) 1206–1234. doi:10.1093/imanum/drn083.
URL https://doi.org/10.1093/imanum/drn083

[16] B. Cockburn, B. Dong, J. Guzmán, M. Restelli, R. Sacco, A hybridizable discontinuous Galerkin method for steady-state convection-diffusion-reaction problems, SIAM J. Sci. Comput. 31 (5) (2009) 3827–3846. doi:10.1137/080728810.
URL https://doi.org/10.1137/080728810

[17] N. C. Nguyen, J. Peraire, B. Cockburn, An implicit high-order hybridizable discontinuous Galerkin method for linear convection-diffusion equations, J. Comput. Phys. 228 (9) (2009) 3232–3254. doi:10.1016/j.jcp.2009.01.030.
URL https://doi.org/10.1016/j.jcp.2009.01.030

[18] N. C. Nguyen, J. Peraire, B. Cockburn, An implicit high-order hybridizable discontinuous Galerkin method for nonlinear convection-diffusion equations, J. Comput. Phys. 228 (23) (2009) 8841–8855. doi:10.1016/j.jcp.2009.08.030.
URL https://doi.org/10.1016/j.jcp.2009.08.030

[19] G. Fu, W. Qiu, W. Zhang, An analysis of HDG methods for convection-dominated diffusion problems, ESAIM Math. Model. Numer. Anal. 49 (1) (2015) 225–256. doi:10.1051/m2an/2014032.
URL https://doi.org/10.1051/m2an/2014032

[20] Y. Chen, B. Cockburn, Analysis of variable-degree HDG methods for convection-diffusion equations. Part I: general nonconforming meshes, IMA J. Numer. Anal. 32 (4) (2012) 1267–1293. doi:10.1093/imanum/drr058.
URL https://doi.org/10.1093/imanum/drr058

[21] Y. Chen, B. Cockburn, Analysis of variable-degree HDG methods for convection-diffusion equations. Part II: Semimatching nonconforming meshes, Math. Comp. 83 (285) (2014) 87–111. doi:10.1090/S0025-5718-2013-02711-1.
URL https://doi.org/10.1090/S0025-5718-2013-02711-1

[22] B. Cockburn, J. Gopalakrishnan, F.-J. Sayas, A projection-based error analysis of HDG methods, Math. Comp. 79 (271) (2010) 1351–1367. doi:10.1090/S0025-5718-10-02334-3.
URL https://doi.org/10.1090/S0025-5718-10-02334-3

[23] W. Eckhaus, Boundary layers in linear elliptic singular perturbation problems, SIAM Rev. 14 (1972) 225–270. doi:10.1137/1014030.
URL https://doi.org/10.1137/1014030

[24] H. Goering, A. Felgenhauer, G. Lube, H.-G. Roos, L. Tobiska, Singularly perturbed differential equations, Vol. 13 of Mathematical Research, Akademie-Verlag, Berlin, 1983.

[25] H. Chen, J. Li, W. Qiu, Robust *a posteriori* error estimates for HDG method for convection-diffusion equations, IMA J. Numer. Anal. 36 (1) (2016) 437–462. doi:10.1093/imanum/drv009.
URL https://doi.org/10.1093/imanum/drv009

[26] H. Zhu, Z. Zhang, Uniform convergence of the LDG method for a singularly perturbed problem with the exponential boundary layer, Math. Comp. 83 (286) (2014) 635–663. doi:10.1090/S0025-5718-2013-02736-6.
URL https://doi.org/10.1090/S0025-5718-2013-02736-6

[27] T. Apel, Anisotropic finite elements: local estimates and applications, Advances in Numerical Mathematics, B. G. Teubner, Stuttgart, 1999.

[28] T. Dupont, R. Scott, Polynomial approximation of functions in Sobolev spaces, Math. Comp. 34 (150) (1980) 441–463. doi:10.2307/2006095.
URL https://doi.org/10.2307/2006095

[29] G. Kunert, Error estimation for anisotropic tetrahedral and triangular finite element meshes, Tech. Rep. SFB393/97-16, Fakultät Mathematik, Technische Universität Chemnitz, Chemnitz, Germany (1997).

[30] F. Hecht, BAMG: bidimensional anisotropic mesh generator. User guide (1998).

[31] B. Cockburn, W. Qiu, M. Solano, A priori error analysis for HDG methods using extensions from subdomains to achieve boundary conformity, Math. Comp. 83 (286) (2014) 665–699. doi:10.1090/S0025-5718-2013-02747-0.
URL https://doi.org/10.1090/S0025-5718-2013-02747-0

[32] H.-G. Roos, M. Stynes, L. Tobiska, Robust numerical methods for singularly perturbed differential equations, 2nd Edition, Vol. 24 of Springer Series in Computational Mathematics, Springer-Verlag, Berlin, 2008, convection-diffusion-reaction and flow problems.

k	N	$e_{\boldsymbol{q}}$	e.o.c	e_u	e.o.c	$e_{\boldsymbol{\sigma}}$	e.o.c	$e_{\widehat{u}}$	e.o.c
0	32	1.98e-01	$--$	4.88e-01	$--$	6.89e-01	$--$	7.07e+00	$--$
	128	7.44e-02	0.41	3.40e-01	-0.48	4.81e-01	-0.48	5.13e+00	-0.54
	512	4.60e-02	0.11	1.79e-01	0.34	2.54e-01	0.34	3.73e+00	-0.12
	2048	3.46e-02	-0.01	9.31e-02	0.53	1.32e-01	0.53	2.68e+00	0.06
	8192	2.87e-02	-0.05	4.88e-02	0.61	6.90e-02	0.61	1.92e+00	0.16
	32768	2.54e-02	-0.09	2.65e-02	0.62	3.74e-02	0.62	1.38e+00	0.21
	131072	2.28e-02	-0.07	1.53e-02	0.57	2.16e-02	0.57	1.00e+00	0.24
1	32	3.25e-02	$--$	2.24e-01	$--$	3.17e-01	$--$	1.74e+00	$--$
	128	1.37e-02	0.24	4.26e-02	1.39	6.03e-02	1.39	7.60e-01	0.19
	512	5.66e-03	0.69	9.57e-03	1.57	1.35e-02	1.57	3.44e-01	0.56
	2048	2.43e-03	0.80	2.24e-03	1.68	3.17e-03	1.68	1.53e-01	0.75
	8192	1.05e-03	0.88	5.33e-04	1.75	7.49e-04	1.76	6.63e-02	0.88
	32768	4.80e-04	0.87	1.25e-04	1.83	1.71e-04	1.86	2.80e-02	0.98
	131072	2.48e-04	0.72	2.76e-05	1.95	3.49e-05	2.07	1.17e-02	1.03
2	32	1.65e-02	$--$	2.67e-02	$--$	3.81e-02	$--$	3.42e-01	$--$
	128	3.00e-03	1.46	2.54e-03	2.40	3.63e-03	2.39	1.18e-01	0.54
	512	6.95e-04	1.52	2.57e-04	2.71	3.71e-04	2.70	3.94e-02	0.99
	2048	1.74e-04	1.58	2.92e-05	2.72	4.34e-05	2.68	1.18e-02	1.32
	8192	4.03e-05	1.78	3.77e-06	2.63	5.91e-06	2.55	3.21e-03	1.55
	32768	8.72e-06	1.94	5.25e-07	2.58	8.73e-07	2.49	8.16e-04	1.71
	131072	2.04e-06	1.87	7.99e-08	2.49	1.41e-07	2.41	1.99e-04	1.81
3	32	9.26e-03	$--$	3.91e-03	$--$	5.68e-03	$--$	7.45e-02	$--$
	128	9.70e-04	2.25	2.18e-04	3.16	3.18e-04	3.15	1.82e-02	1.03
	512	1.62e-04	1.99	1.54e-05	3.23	2.38e-05	3.15	4.98e-03	1.28
	2048	2.68e-05	2.18	1.37e-06	3.07	2.61e-06	2.77	1.03e-03	1.86
	8192	3.66e-06	2.55	1.63e-07	2.75	3.38e-07	2.62	1.77e-04	2.22
	32768	4.16e-07	2.87	1.96e-08	2.78	4.09e-08	2.78	2.70e-05	2.44
	131072	3.75e-08	3.24	2.20e-09	2.93	4.48e-09	2.97	3.85e-06	2.59

Table 5: History of convergence of Example 5. $\epsilon = 10^{-3}$.

N	$k=0$	$k=1$	$k=2$	$k=3$
32	3.80e+04	2.69e+04	2.19e+04	1.90e+04
128	2.69e+04	1.90e+04	1.55e+04	1.34e+04
512	2.19e+04	1.55e+04	1.27e+04	1.10e+04
2048	1.90e+04	1.34e+04	1.10e+04	9.50e+03
8192	1.70e+04	1.20e+04	9.81e+03	8.49e+03
32768	1.55e+04	1.10e+04	8.95e+03	7.75e+03
131072	1.44e+04	1.02e+04	8.29e+03	7.18e+03

Table 6: $\max_{K\in\mathcal{T}} \left(\frac{h_K}{h_{\min,K}}\right)^{1/2}$ for meshes of Example 5 with $\epsilon = 10^{-9}$.

k	N	$e_{\boldsymbol{q}}$	e.o.c	e_u	e.o.c	$e_{\boldsymbol{\sigma}}$	e.o.c	$e_{\widehat{u}}$	e.o.c
0	32	1.94e-01	$--$	4.88e-01	$--$	6.90e-01	$--$	6.28e+03	$--$
	128	6.55e-02	0.56	3.39e-01	-0.47	4.80e-01	-0.47	4.36e+03	-0.47
	512	3.57e-02	0.29	1.77e-01	0.35	2.50e-01	0.35	3.12e+03	-0.11
	2048	2.25e-02	0.25	9.00e-02	0.56	1.27e-01	0.56	2.23e+03	0.07
	8192	1.39e-02	0.37	4.53e-02	0.67	6.41e-02	0.67	1.59e+03	0.17
	32768	8.29e-03	0.48	2.28e-02	0.73	3.22e-02	0.73	1.13e+03	0.23
	131072	4.80e-03	0.57	1.14e-02	0.77	1.61e-02	0.77	8.03e+02	0.27
1	32	1.15e-02	$--$	2.25e-01	$--$	3.19e-01	$--$	1.29e+03	$--$
	128	7.59e-03	-0.39	4.32e-02	1.38	6.11e-02	1.38	6.75e+02	-0.07
	512	3.88e-03	0.38	9.85e-03	1.55	1.39e-02	1.55	3.26e+02	0.47
	2048	1.66e-03	0.81	2.36e-03	1.65	3.34e-03	1.65	1.48e+02	0.72
	8192	6.42e-04	1.05	5.77e-04	1.71	8.17e-04	1.71	6.43e+01	0.88
	32768	2.33e-04	1.20	1.43e-04	1.75	2.02e-04	1.75	2.69e+01	0.99
	131072	8.01e-05	1.32	3.55e-05	1.78	5.02e-05	1.78	1.10e+01	1.07
2	32	6.41e-03	$--$	2.64e-02	$--$	3.74e-02	$--$	2.00e+02	$--$
	128	1.56e-03	1.04	2.51e-03	2.40	3.54e-03	2.40	1.05e+02	-0.07
	512	5.27e-04	0.98	2.55e-04	2.71	3.61e-04	2.71	3.84e+01	0.86
	2048	1.42e-04	1.48	2.85e-05	2.75	4.03e-05	2.75	1.18e+01	1.29
	8192	3.36e-05	1.76	3.39e-06	2.75	4.80e-06	2.75	3.20e+00	1.56
	32768	7.06e-06	1.99	4.16e-07	2.77	5.88e-07	2.77	8.05e-01	1.73
	131072	1.40e-06	2.12	5.15e-08	2.79	7.28e-08	2.79	1.92e-01	1.85
3	32	7.35e-04	$--$	3.92e-03	$--$	5.54e-03	$--$	3.49e+01	$--$
	128	5.30e-04	-0.53	2.20e-04	3.16	3.11e-04	3.16	1.78e+01	-0.03
	512	1.47e-04	1.27	1.50e-05	3.29	2.12e-05	3.29	5.00e+00	1.25
	2048	2.64e-05	2.06	9.57e-07	3.55	1.35e-06	3.55	1.04e+00	1.86
	8192	3.73e-06	2.50	6.04e-08	3.66	8.54e-08	3.66	1.77e-01	2.22
	32768	4.73e-07	2.71	3.79e-09	3.73	5.36e-09	3.73	2.70e-02	2.46
	131072	8.40e-08	2.27	2.37e-10	3.77	3.36e-10	3.77	3.82e-03	2.59

Table 7: History of convergence of Example 5. $\epsilon = 10^{-9}$.